Controlling Pillow Defect in Single Point Incremental Forming Through Varying Tool Geometry

Besong Besong Lemopi Isidore

Submitted to the
Institute of Graduate Studies and Research
in partial fulfillment of the requirements for the Degree of

Master of Science
in
Mechanical Engineering

Eastern Mediterranean University
June 2014
Gazimağusa, North Cyprus

Approval of the Institute of Graduate Studies and Research

Prof. Dr. Elvan Yilmaz
Director

I certify that this thesis satisfies the requirements as a thesis for the degree of Master of Science in Mechanical Engineering.

Prof. Dr. Uğur Atikol
Chair, department of Mechanical Engineering

We certify that we have read this thesis and that in our opinion it is fully adequate in scope and quality as a thesis for the degree of Master of Science in Mechanical Engineering.

Asst. Prof. Dr. Khalid A. Al-Ghamdi
Co-supervisor

Asst. Prof. Dr. Ghulam Hussain
Supervisor

Examining Committee

1. Assoc. Prof. Dr Hasan Hacişevki
2. Asst. Prof. Dr.Ghulam Hussain
3. Asst. Prof. Dr. Mostafa Ranjbar

ABSTRACT

Single point incremental forming (SPIF) is a new sheet forming process with much potential for application in industry and can be used in combination or in place of standard sheet forming processes. However, part accuracy is a major drawback in this process. Pillow formation in particular is a major defect in SPIF because it leads to early fracture and part inaccuracy.

This study aims at understanding the effects of sheet thickness, tool geometry and radius on pillowing in SPIF. The study was carried out on aluminum 1060 alloy (commercial aluminum).The findings are determined based on practical work and simulations using Finite Element Analysis (FEA) on Abaqus 6.12. The temperature, machining conditions and material property are assumed to be same in FEA.

Parameters that influence the formation of pillow were studied. It is observed that an increase in tool radius decreases pillow height due lower stresses and strains as revealed by FEA. Flats tools tend to form lower pillows than round tools due to lower bending angles and also the fact that flat tools may bend the sheet at two points along the profile. Pillow height was found to increase with sheet thickness. The ratio of the tool size to sheet thickness was proven to be a very important parameter as this determines the amount of bend severity. FEA was used to determine of the stress and strain states in SPIF and hence an explanation for pillowing mechanism. The results are expected to be a useful reference to designers and manufacturing enterprises.

Keywords: Single Point Incremental Forming, Pillow Forming, Small batch production, Finite Element Analysis, Modeling, Part Accuracy.

ÖZ

Tek noktalı artan şekillendirme, endüstride kullanım potansiyeli çok ve kombinasyonlarla veya standart levha şekillendirmenin yerine kullanılan bir işlemdir. Parça doğrultu bu işlemin en büyük dezavantajıdır. Yastık oluşumu bu işlemin en büyük hatasıdır çünkü erken kırılma ve parça eğrilmesine sebep olur.

Bu çalışma, levha kalınlığının, olet geometrisinin ve yastiklama işlemindeki yarı çapın, tek noktalı artan şekillendirmeninü zerindeki etkisini ortaya koyar. Bu deney, 1060 alüminyum alaşım üstünde gerçekleşti. Buluşumlar, pratik iş ve sonlu elemar analizini kullarak ortaya akmıştır. Sıcaklık, işleme şartları ve material özellikleri, sonlu elemar analizi ile aynı olduğu var sayıldı.

Yastık üretimindeki parametrelerin etkileri araştırıldı. Sonu elemar analizinde ortaya çıkan gerilim ve burkulmaya bağlı olarak, alet yarı çapı azaldığında yastık yüksekliğinin de azaldiği gürülmşütür. Düz aletin levhayi bükmesi ve düşük bükme açılarına bağlı olarak düz aletler, yuvarlak aletlere oranla daha alçak yastıklar üretilir.

Levha kalınliğına bağlı olarak yastık yüksekliğinin artması gözlemlendi. Bükülme derecesini saptamak için kullanırlar, alet boyutunun levha kalınlığına oranının, çok önemli bir parameter olduğu kanıtlarımıştır. Sonlu eleman analizi, tek noktalı artan şekillendirme de belirtilen bükülme ve gerilmeyi bulmak için kullanılır ve ayrıca yastıklama mekanizması için bir açıklamadır. Çıkan sonuçlar, tasarım ve üreticiler için kullanışlı referanslar olması beklenir.

Anahtar kelimeler: Tek noktalı artan şekillendirme, Yastık oluşumu, küçük ölçekli üretim, sonlu eleman analizi, modelleme, parça doğruluğu.

DEDICATION

To my family;
My mum Florence, my siblings Goretti, Anyim, Mirabeau and Ross

ACKNOWLEDGMENT

I would like to sincerely thank my thesis supervisor Assist. Prof. Dr. Ghulam Hussain for introducing me to incremental forming and for the many contributions he has made during the course of my studies and the writing of this thesis. I would like to thank Asst. Prof. Dr. Khalid A Al-Ghamdi for his financial support and contributions during the course of writing this thesis. I very much appreciate the efforts made by Assoc. Prof. Dr. Hasan Hacışevki, Asst. Prof. Dr. Mostafa Ranjbar in reading and correcting this thesis. I would also like to express sincere thanks to Prof. Dr. Uğur Atikol, Asst. Prof Dr. Gohkan Izbirak and Asst. Prof Dr. Sahand Daneshvar for the support they gave me during the course of my studies. I specially thank Mr Khosro Bijanrostami and Hosein Khalibari for their assistance and contributions they made in the realization of the practical part of this thesis. I like to remember the moral support of my teachers, friends and colleagues. I would like to express great appreciation to my family: my mother, sisters and my brothers for their endless love. Not forgetting Mbah, Ayoola, Jaiyaejej, Gopti, Sahand, Asabs, Stanley and Ridley. I will never forget your support.

TABLE OF CONTENTS

LIST OF TABLES

LIST OF FIGURES

LIST OF SYMBOLS AND ABBREVIATIONS

Abbreviations /symbols	Meaning
SPIF	Single Point Incremental Forming
DPIF	Double Point Incremental Forming
TPIF	Two Point Incremental Forming
MPF	Multi-Point Forming
FEA	Finite Element Analysis
CAM	Computer Aided Manufacturing
CAD	Computer Aided Design
INP file	Input File
CL	Cutter Location
CNC	Numerical Control
3D	3 Dimensions
Al	Aluminum
Fe	Iron
Cu	Copper
Mg	Magnesium
Mn	Manganese
Ni	Nickel
Zn	Zinc
Ti	Tin
Si	Silicon

Chapter 1

INTRODUCTION

1.1 Problem statement

Metal sheet forming is a major manufacturing process used to manufacture many products in various branches of industry. With technological advancements, products with complex shapes can be made by deforming clamped sheets with the help of tools, which have been programmed to move along the profile of a desired shape. Large production batches can cover up the cost of expensive dies and tooling required in conventional sheet metal working processes, however, for small and medium sized batches of production conventional processes like deep drawing and stamping are very expensive because of the few parts involved.

Single products such as prototypes are used during the development or improvement of a design in most manufacturing industries. This permits evaluation of a design and reduction of product development time. A prototype typically requires a lot work from skilled personnel in manufacturing, coupled with the slow rate and the trial and error method often used in the try out designs [1]. Additionally, the investment cost and time consumed in producing dies, forming prototypes and preproduction of parts using conventional processes is too expensive. Therefore, there is the need for cheaper means to produce sheet metals part which are often needed in small quantities.

More customers and enterprises want to carryout business with enterprises that produce green products and use green manufacturing. Energy efficiency in the manufacturing sector is a major factor that affects global energy demand and contributes to the impact of manufacturing on the environment. Actually manufacturing accounts for about 31% of primary energy usage and 36% of carbon dioxide (CO_2) emissions [1]. Energy efficiency in manufacturing has a considerable value on a products' environmental impact assessment and this is becoming a major driver for competiveness. There is a high flexibility associated with single point incremental forming as modifying the input program leads to a new product. Implying many products may require same set of equipment in their manufacturing procedure. The cost on the environment of disposing equipment associated with this kind of manufacturing technique is negligible. Single point incremental forming typically requires lower energy demand than standard manufacturing processes.

With the advent of international trade and the free market economy, enterprises need to be more innovative, develop new products and produce more complex products at cheaper prices from very limited resources. Customers have a varying demand for products with an accompanying high taste. This means enterprises have to create loyalty among customers to brand names as well as implement mass customization. Mass customization requires more production lines; however with the use of single point incremental forming more products can be manufactured using the same equipment in order to reduce cost.

Enterprises are faced with steeper competition in the market from rivals. In order to survive this competition, the individual needs of customers must be satisfied. This

involves a lot of changes in the design and manufacturing stage in a product's life cycle.

Single point incremental forming can satisfy such needs because of the small changes needed in the design and manufacturing process. As such it is ideal for small and medium sized enterprises which often produce 'one of a kind product' that typically require much time, changes in design, fixtures and manufacturing.

1.2 Purpose

The aim of this thesis is to better understand the influence of the tool radius and geometry (flat or round) tool on the formation of a pillow at the center of the blank during in (SPIF), which has major influences on premature fracture and defects on the product. The mechanism of bulge formation is studied to propose how to prevent bulge formation.

Other objectives of the thesis include analyzing the influence of sheet thickness on pillow formation in single point incremental forming. The influence of process variables like forming angle, step size and lubrication are also discoursed. However, they are kept fixed during the course of the experiments. The study is carried out on Al 1060-O (commercial Aluminium annealed). The tendencies found out from the experimental work are verified using (Finite Element Analysis) F.E.A simulation on ABAQUS 6.12.1 platform to explore causes of experimental findings and mechanism of pillowing.

1.3 Organization of the Thesis

This thesis is divided into 6 chapters. There is a literature review in chapter two on sheet metal forming processes. Chapter three covers literature review on single point

incremental forming taking into consideration relevant process parameters and discoursing their effects. Chapter four presents experiments, simulations, data collection methods and the presented model. The material preparation, machine tools, geometry of the tools and simulation parameters are found in chapter four. The experiments and FEA simulation results obtained are presented in chapter five. Lastly chapter six includes a conclusion and suggestions for future research in this area.

Chapter 2

INCREMENTAL FORMING PROCESSES

2.1 Introduction

In this chapter we review incremental forming processes taking into consideration recent applications in terms of variability, formability, applicability and materials on which they are performed. Other configurations of Single Point Incremental Forming (SPIF) are also discussed.

2.2 Incremental Forming Processes

2.2.1 Flow Forming

Tube spinning (flow forming), is a manufacturing method closely linked to forming by shearing of the material. The part being formed is rotated while a tool displaces the material on a mandrel, there is no variation in the dimension of the internal surface. Three or two rollers are used in most flow forming equipment and their design is more complex compared to that of spinning and shear forming machines.

During the process, both the mandrel and blank are rotated while the spinning tool contacts the blank and progressively induces a change in its shape according to the profile of the mandrel. Two techniques are used for metal tube spinning, backward and forward tube spinning, demonstrated in the figure below. The travel of the roller in relation to the material (part) determines the type of forming process.

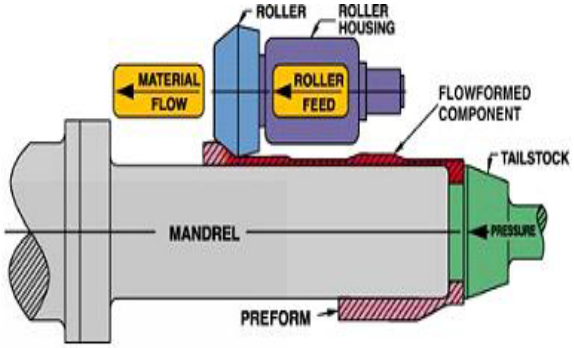

Figure 2.1: Forward flow forming [2]

In reverse spinning the work piece is fixed on the head stock with the use of a fixture and a roller moves towards the work piece clamped part, work flows in the opposite direction as in figure [2.2].

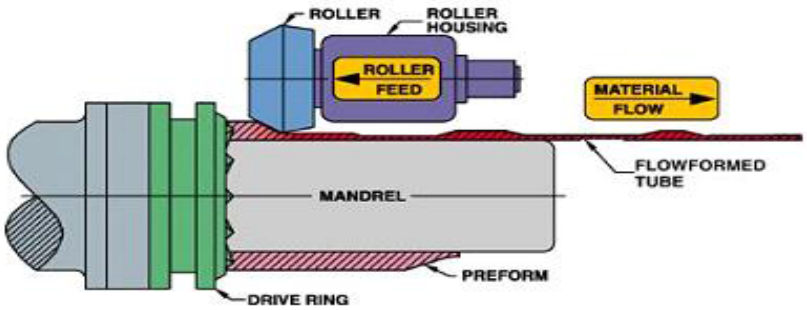

Figure 2.2: Reverse flow forming [2]

2.2.2 Hammering

Incremental sheet forming by hammering is one of the oldest kinds of incremental sheet forming. With the growth of technology, the use of programmable machines such as CNC machines have eliminated manual work and also increased levels of production and accuracy. The sheet is fixed on a fixture and a robot arm is used to control the tool's movement. There is no die below the clamp so the sheet is deformed by the stresses created by the tool. Hammering is done following a predetermined path and the blank takes the shape of the desired part to be produced

as in figure 2.3. For some geometries, the parts being formed have to be rotated and shaped in several steps to obtain the desired shape.

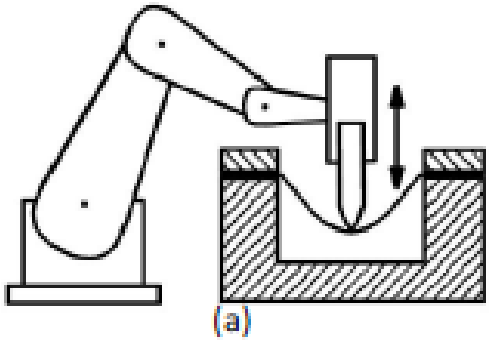

Figure 2.3: Sheet forming by hammering [3]

2.2.3 Laser Forming

Unlike conventional manufacturing techniques, laser forming does not require mechanical contact and hence has more process flexibility and can perform other processes such as laser cutting and marking. The surface to be deformed is heated with a laser as thermal stresses are introduced into work piece. This rise in temperature causes reduction in internal strains in the material and as a result localized buckling occurs deforming the material to a new shape.

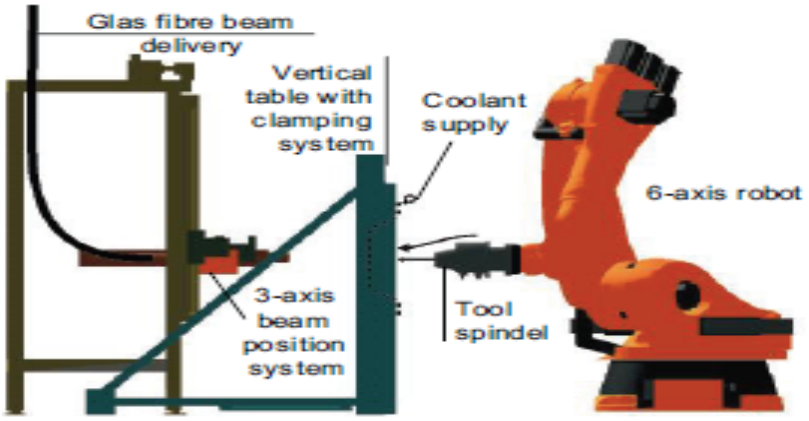

Figure 2.4: Single point incremental forming with dynamic, laser supported heating [4]

Laser forming shown in figure 2.4 has been used to replace processes that previously relied mostly on expensive presses and dies for prototype manufacture and evaluation. Sectors of industry that typically use this process include aerospace, automotive, and microelectronics.

Costs related with the forming stand, the need for highly skilled personnel, high energy consumption, personnel safety equipment and the pre-coating of the metal sheet as the need arises in order to increase the absorbance are disadvantages hindering the use of this process in industry. Some of these problems were successfully solved by replacing the laser by plasma arc [5].

2.2.4 Water Jet Machining

Similar to laser jet forming, water jet forming deforms the surface of the blank locally by inducing stresses in areas in contact with the water jet. There is dislocation in the areas of the sheet surrounding the stressed part and as a result the sheet is deformed to the required shape. As advantages, we have: more flexibility, better surface quality, less tooling is needed, low cost of equipment and less harm to the environment. On the other hand, water jet forming is less accurate, consumes more energy and takes more time than the other incremental metal forming processes [6].

2.2.5 Sheet Spinning

Sheet spinning is accomplished by rolling an axis-symmetrically shaped part progressively over a mandrel using a blunt tool usually round or a roller. This process is often very cost effective and large parts can be manufactured using this method. However, only axis-symmetric parts can be manufactured using this method and usually only small batches of production are possible.

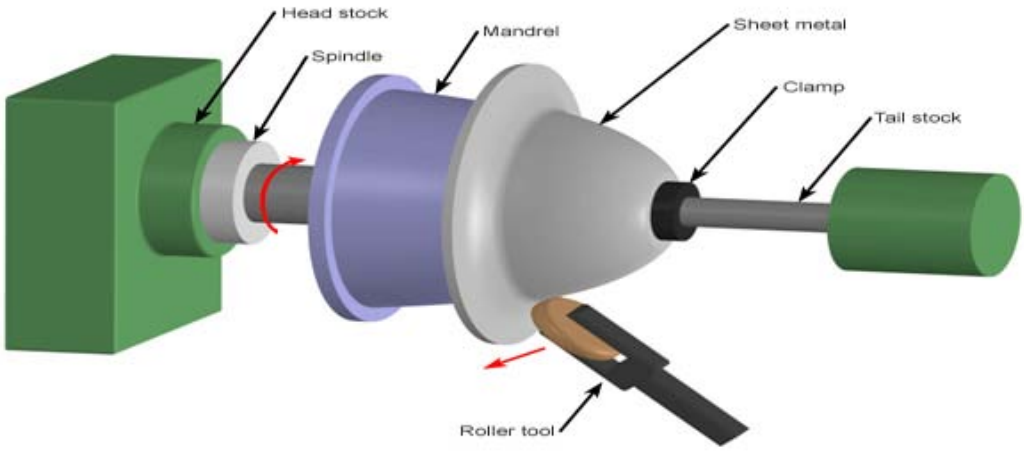

Figure 2.5: Sheet spinning operation [7]

There are basically two kinds of spinning: Conventional spinning and Shear spinning.

In conventional Spinning, axis-symmetric parts are formed gradually over a wooden or plastic mandrel with the use of a tool. The work piece is set on the lathe and deformed by a round tool. The pressure applied by the tool is localised and deforms the sheet axially and along the direction of the radius. The tool motions can be manually or automatically programmed. The deformation is performed in several steps and large stretches can be achieved as in figure 2.5.

In shear spinning the sheet is stretched instead of bent. The length of the final piece is approximately equal to the length of the original work piece. The thickness of the piece can be controlled by maintaining the distance separating the tool and rotating arbor. The thickness of the blank reduces as it is formed as in figure 2.6. This variation can be gotten using the sine law below.

$$t_f = t_i \sin\alpha \tag{2.1}$$

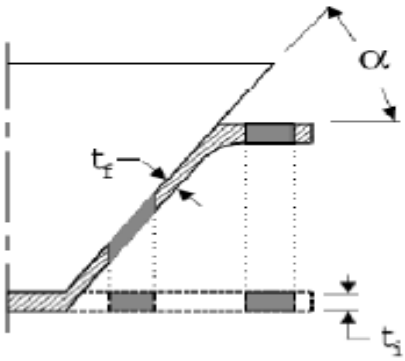

Figure 2.6: Deformation of an element in a shear formed cone [8]

2.2.6 Shot Peen Forming

In this process, the blank's surface undergoes impacts from a small round steel ball. Every impact on the surface of the sheet produces local stresses in the blank and acts as a form of hammering. Tensile and compressive forces acting on the sheet's side undergoing impacts causes it to deform to the required shape. Steel balls are often forced out of a nozzle and causes static stresses in the areas where they come in contact with the sheet, see figure 2.7. Shot peen forming can be used to form large panels with a large radius and no abrupt changes in contour such as in parts used in the aerospace industry. Research on double-sided simultaneous shot peen forming was carried out by, [9] to improve productivity, applications and formability.

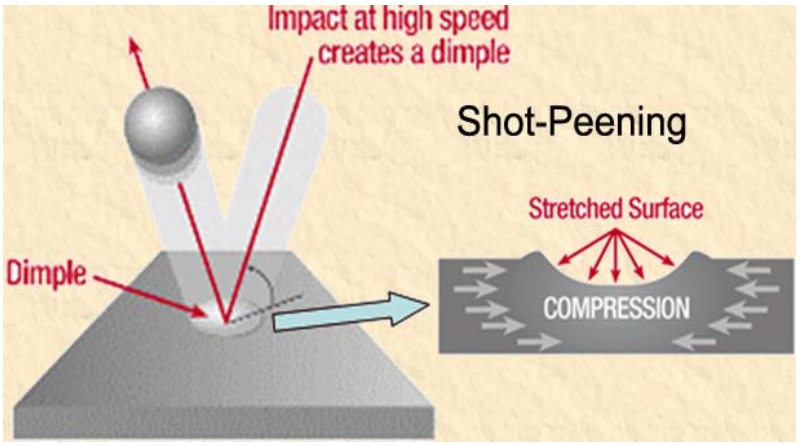

Figure 2.7: Shot peen forming [10]

2.2.7 Multi Point Forming

In Multi-point Forming (MPF) panels are produced in a very similar fashion to the forming processes that use solid dies. In conventional forming processes, two opposite solid parts are used to deform a blank to the required geometry corresponding to the required shape of the product being produced. In MPF technology the solid die is replaced by several punches which are adjustable to specific heights using actuators [11, 12], this enables changes in the shape of the dies to different shapes without too much time consumption, this is shown in Figure 2.8 below.

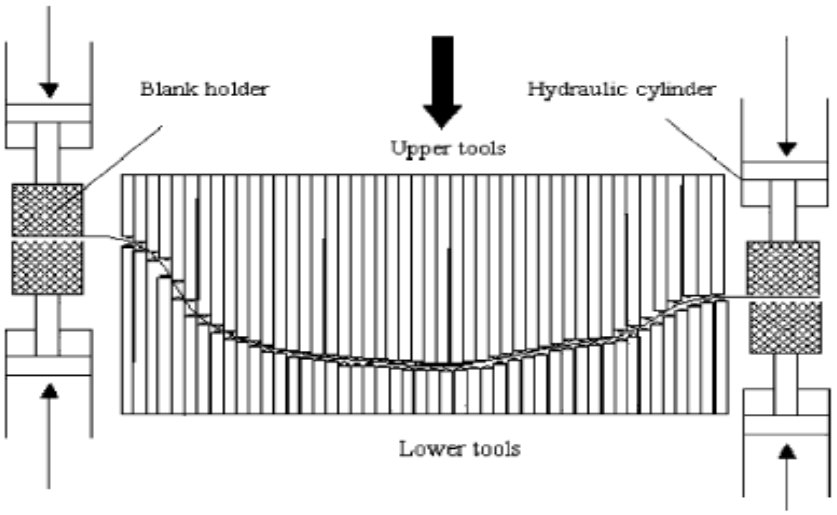

Figure 2.8: Metal sheet forming using programmed tools to form the sheet at multiple points [11]

2.3 Multi Stage Forming Process

Due to thinning of the blank that occurs as a sheet is being deformed, multi stage forming processes have been implemented to reduce the effect of sheet thinning. For a sheet with a specific thickness and material composition there is a maximum angle at which deformation can occur without failure. Factors such as step size and tool diameter can be kept constant to determine this maximum angle. When the maximum

forming angle has been attained for a given blank, failure occurs. An increase in blank thickness increases the maximum wall angle but this strategy is limited by the machine load and part specifications. Tool diameter and step size also play an important role on the maximum forming angle [13]. We can alternatively obtain large wall angles through moving to the formed walls from different areas of the part.

Previous researchers have adopted different strategies for multistage forming. Consecutive tool paths have been implemented using many steps method to deform a part using increasing tool path angles. The first path requires a great offset to prevent extreme strains on the top and bottom surface of the part at the point of contact with the support and permit to more bending of the part. Also in order to overcome this limitation some researchers [14] applied multiple stages strategies with success (using pre-forms), shown in figure 2.9 below. Although forming using a multi stage strategy can effectively reduce the problem of thinning, however, reducing thinness thickening has not been solved and there is no specific law governing sheet thinning and what is the right procedure to follow for each forming process.

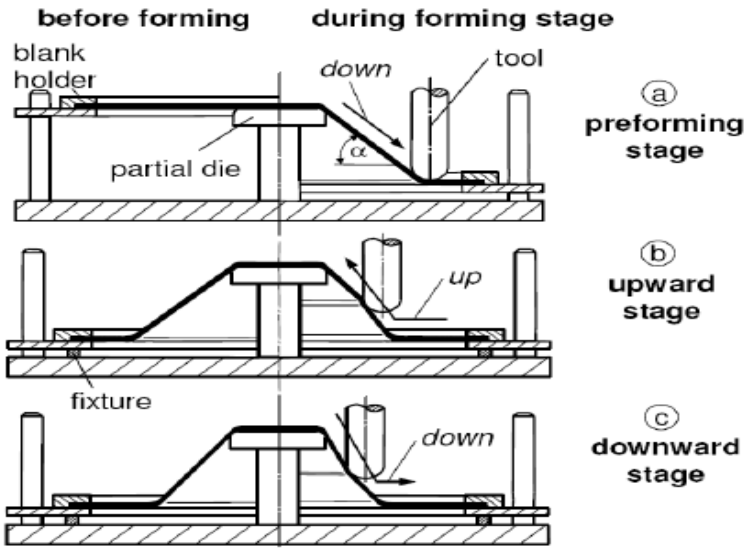

Figure 2.9: Single point multistage strategy [15]

2.4 Point Incremental Forming Processes

2.4.1 Double Point Incremental Forming (DPIF) Process

DPIF is a method used to form a blank in which the part is clamped to a blank holder. The tool or support can be moved along the z direction. The tool's motion is programmed along the outer surface of the blank. The part is manufactured from the bottom to the top. Two types of TPIFs exit: partial die and full die TPIF.

2.4.2 Double Point Incremental Forming

A partial die is used in this process as a back plate. It acts as a support on the blank's opposite side in the areas where the tool makes contact, thereby increasing geometrical accuracy, shown in figure 2.10 below. Partial dies could be used to make parts which are geometrically similar.

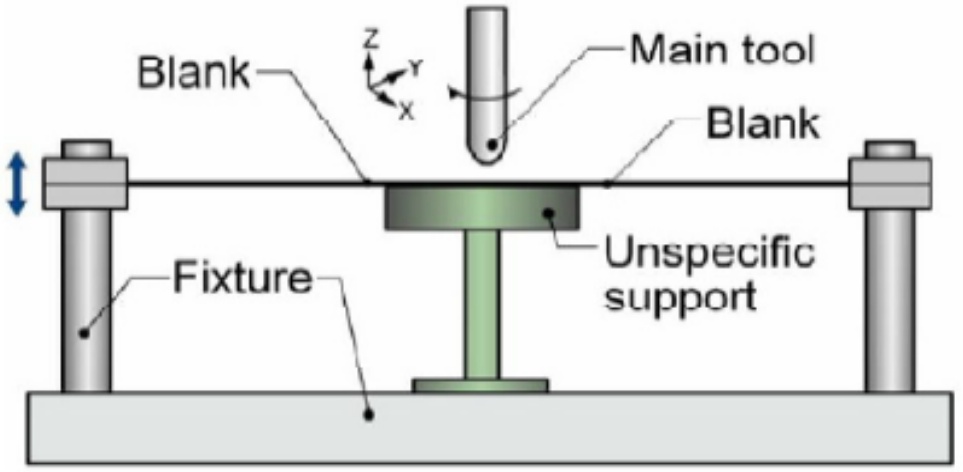

Figure 2.10: Double Point Incremental Forming (partial die) [16]

2.4.3 Double Point Incremental Forming (DPIF) full die

Often (DPIF) is not accepted as dieless forming as it is done with two dies, as in figure 2.11. It can produce parts with good geometrical accuracy since the part is prevented from moving between the forming equipment (die and tool).Disadvantages of DPIF with a full die include high cost of the die material (often steel, aluminium,

wood, plastic or form) and fabrication. Flexibility is also reduced since a new blank is required for each product.

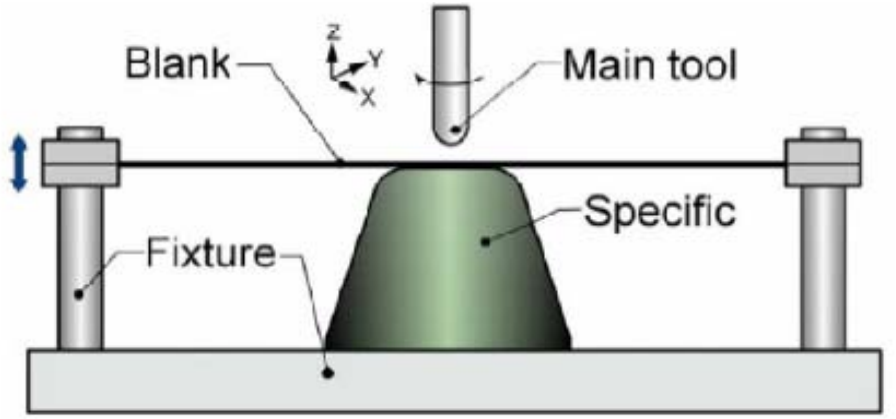

Figure 2.11: Double Point Incremental Forming (full die) [16]

2.4.4 Incremental Forming With a Counter Tool (IFWCT)

In IFWCT a tool is used on the opposite side of the blank instead of a back plate. The auxiliary tool follows the path as the main tool, see figure 2.12. Local stresses and strains can be control by the actions of both tools. This leads to better out puts as the process is better controlled. The process is shown in the diagram.

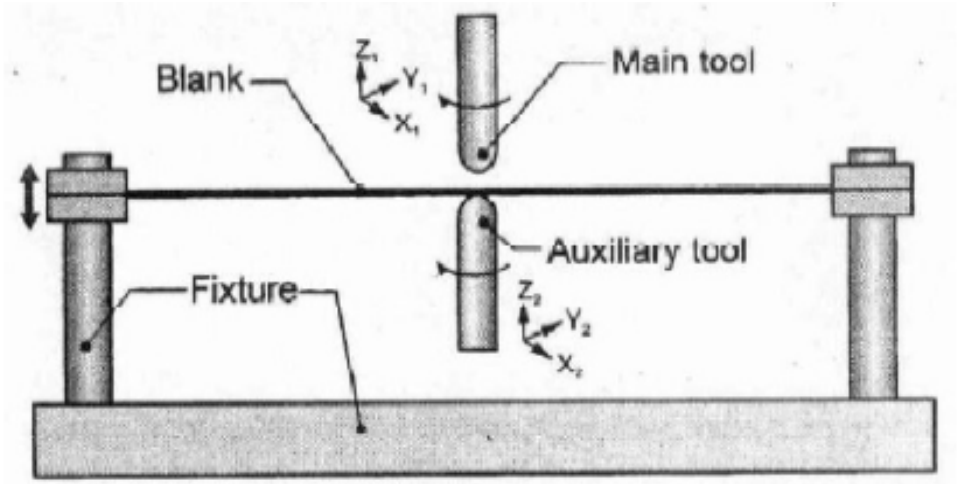

Figure 2.12: Schematic representation of Incremental Forming with Counter Tool [17]

2.4.5 Single Point Incremental Forming (SPIF)

In SPIF, a part is formed using several steps to deform a sheet (blank) in layers as in figure 2.13. The sheet is deformed locally by a tool usually round. The tool moves in a pre defined path programmed by using soft ware. The tool path is created with the help of a Computer Aided Design soft ware (CAD software) and Computer Aided Manufacturing software (CAM). The tool moves on a blank which is firmly clamped at the edge using a stand. The main steps of SPIF process are shown in the diagram below.

i) The blank is clamped firmly on a stand.

ii) The tool makes contact with the sheet.

iii) The tool moves on the predefined path usually a circular path in steps or spiral motion as the case may be.

iv) The motion is repeated until the steps come to an end.

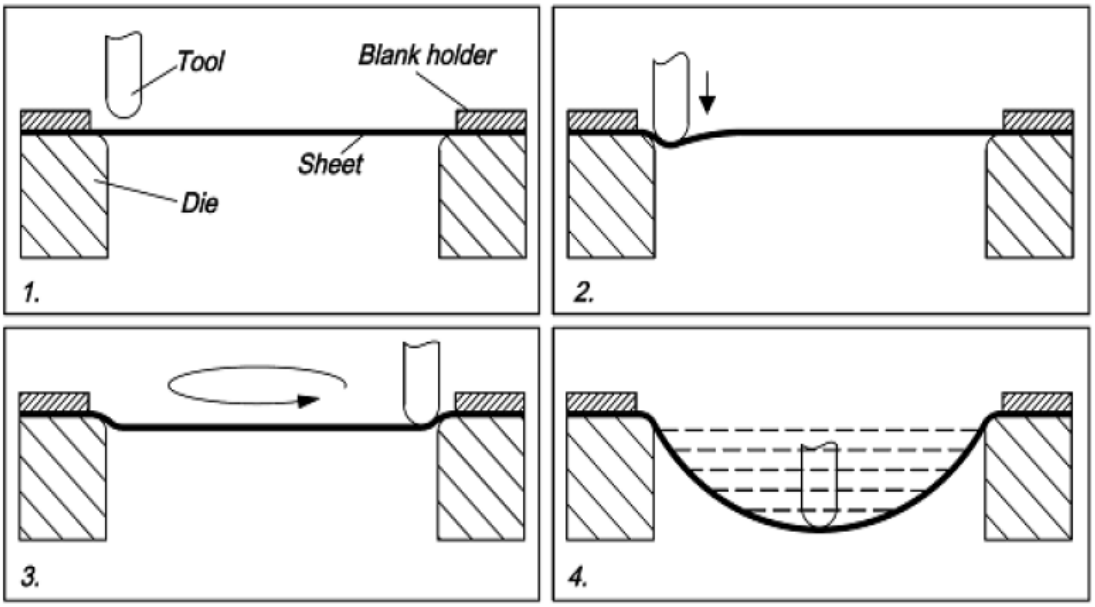

Figure 2.13: Main stages in SPIF [18]

Advantages of SPIF over other incremental forming processes:

- Direct production of parts from computer aided drawings.

• Less costly since no positive and negative dies are required.

• Changes can be easily and quickly performed on the design.

• Increased formability of materials.

• Can be carried out on most CNC machine tools.

• Smaller forming forces are required due to localised deformation and incremental application of forming forces.

• Parts to be formed are limited by the dimension of the CNC machine.

The main disadvantages of the SPIF Process are:

• Forming time is long compared to conventional Deep Drawing Process.

• Limited to small production batches and prototype development.

• Many processes are required to form parts with geometry 90^0 degree.

• Spring back occurs after deformation by the tool; therefore formed parts are usually not as accurate as intended in the design phase.

• Less geometrical accuracy, particularly in convex radii and bending edges areas.

2.5 Applications of Incremental Forming Processes

SPIF has two main areas of application in industry.

2.5.1 Automobile Industry

Prototype development, testing and manufacturing are an essential step in the development or improvement of a part before beginning mass production. It allows for a preliminary evaluation of the product during the design stage and a reduction in product development time. For example, automotive industries need to produce about 40-50 critical panels per car model, see Figure 2.14. This requires at least 150-200 dies for the stamping process. Thus, a huge amount of work in the prototype manufacturing process for these dies is needed. [19] The figures below illustrate sheet metal parts of a car. These can be manufactured using incremental forming.

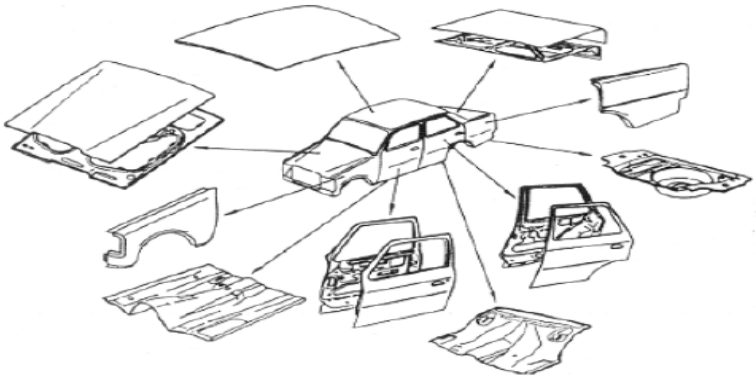

Figure 2.14: Metal sheet parts in major panels of car body [20]

2.5.2 Non Automobile Applications

The following parts can be realised using SPIF: motorbike seats, motorbike gas tanks, solar oven, production dies and mould surfaces.

2.5.3 Some Medical Applications of SPIF include

A B

Figure 2.15: A) Cranial plate B) Dental plate [20]

Other applications of SPIF include home appliances, architectural use, use in aerospace and maritime industry.

2.6 Others Materials

In recent years more aerospace and biomedical applications of SPIF have been developed. [19] Proved that SPIF process could be used to manufacture a dental plate of pure titanium, see Figure 2.15 (b), the main problems during production arose from the surface quality, there was need to find an optimal combination between

lubrication, feed speed and rate. [21] Applied SPIF on commercially pure titanium with the use of proper tools, good lubricant and lubrication method. [22] Proved the viability of manufacturing parts using sandwich panels. These panels are used in large quantities in airplane interior components, automobile panel parts and various applications in architecture where saving weight is important, absorbing sound, impacts, vibrations, and thermal isolation. Formability of commercial PVC (Polyvinyl Chloride) was characterized and evaluated by [23] and came to the conclusion that SPIF could attain very high depths for complex PVC parts manufactured at normal temperatures of complex polymer sheet components. Applications of polypropylene (PP) in SPIF were performed by [24] and several different geometries were studied. [25] Verified the possibility of manufacturing parts by Multistage SPIF of Magnesium AZ31 parts at warm temperatures, and found that formability increases with increase in forming temperature. Magnesium alloy is formable at warm temperatures due to its brittleness. More research should be carried out on due structural applications as it possesses high strength-to- weight ratio.

Chapter 3

LITERATURE REVIEW

3.1 Pillow Formation

Pillow formation is a major geometrical defect in SPIF. Many researchers have attempted solutions to raise geometrical specifications of products made using SPIF. Tool path compensation methods have been used by [26], stress relief annealing was proposed by [27], finite element modeling (FEM) to predict and improve the geometry of the part was proposed by [28], using high temperatures during SPIF has been used by [29], statistical methods have been utilized by [30] to determine how forming parameters influence SPIF. Amongst proposed solutions to obtain better part accuracy, Laser Assisted Single Point Incremental Forming (LASPIF) has been shown to possess highest potentials in obtaining improved accuracy. The area of contact between the sheet and tool is heated synchronously with the movement of the tool. This improves ductility of the material at that point and reduced spring back of the blank. Also the forming stresses are low and there is a low tendency for the deflection of the tool and machinery from the required tool path.

Bulge (pillow) formation at the center of the blank is more pronounced for shallow geometries than for parts formed at angles close to their maximum forming angle. Pillow formation (pillowing) often induces increased forming forces which lead to more inaccuracies in specifications of the part being formed. Experiments carried out by [31] demonstrate that increased tool radius and wall angle hinder pillow formation

(pillow height). Figure 3.1 below shows profile inaccuracy (the deviation of the produced part from the C.A.M design).

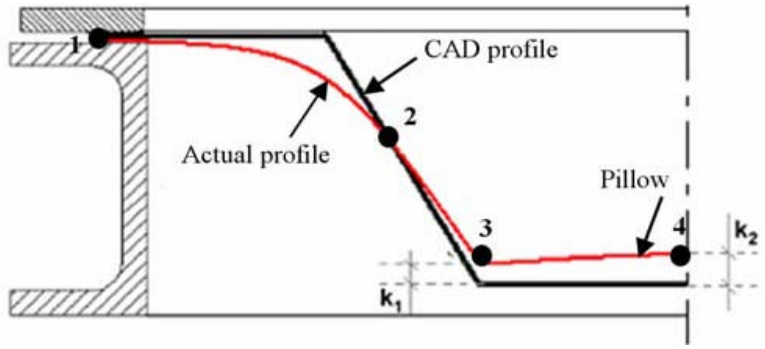

Figure 3.1: Actual cross section of part versus CAD profile [32]

Strains in the plane caused by stresses along the plane in the horizontal are responsible for pillow formation as proposed by [33]. Large step size favors bulge formation because of increased in-plane stresses which increase bulge formation [34]. A decrease in hardening exponent causes a reduction in formability [34].

The thickness of a sheet influences formability based on the hardening law obeyed by the sheet. For blanks having small values for hardening exponent (0.04), pillow height reduces with increased sheet thickness [34]. Bulging in thin sheets seem to be caused by buckling of the sheet rather than deformation related to in plane stresses along the horizontal. For sheets with high hardening exponent, pillow height increases with increased sheet thickness due to increased in-plane stresses.

Consider the section of the sheet undergoing deformation in region A in the figure 3.2 below. The sheet is deformed by a combination of bending and stretching. If bending occurs at a small angle (with no stretching), the middle surface can be taken as neutral surface.

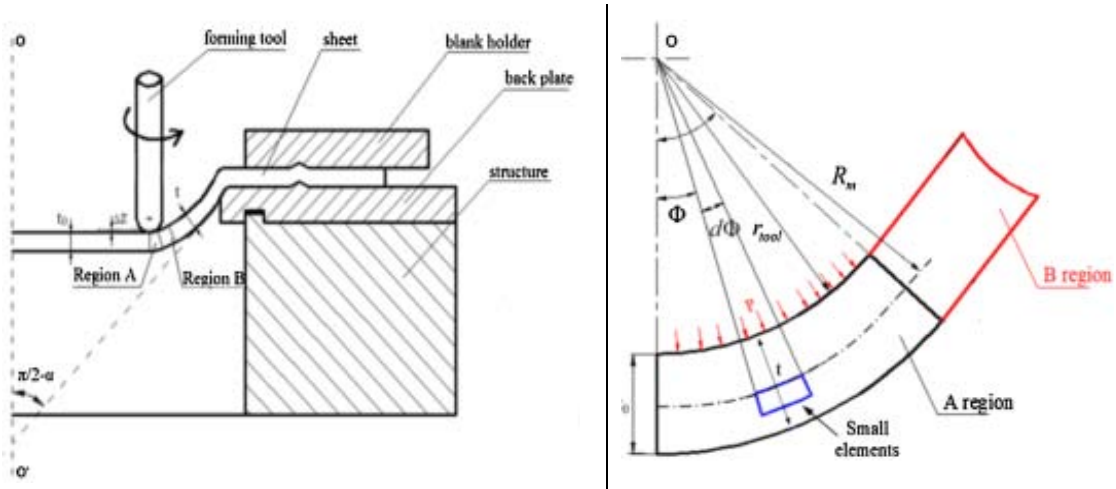

A B

Figure 3.2: Schematic representation of a cross section view of single point incremental sheet forming: (A) overview; (B) detailed view [35]

The surface in contact with the tool is under tensile strain by stretching and compression due to bending. The outer surface is undergoing tensile strain by stretching and tensile strain by bending. If deformation due to bending is not taken into account, the tensile strain as a result of stretching can be represented by the strain at the middle plane of the blank sheet [35]. If we consider the tangential strain ε of the mid plane to be zero, the tensile strain due to stretching can be determined using (3.1) below.

$$\varepsilon_{stretching} = -\varepsilon_t^{mid} = In\frac{t_0}{t} \tag{3.1}$$

Where $-\varepsilon_t^{mid}$ is the strain at the mid surface (thickness strain) and t signifies the thickness of the sheet at a certain angle. Under plane strain conditions, strains as a result of pure bending can be obtained using [36].

$$\varepsilon_A = \varepsilon_{bending} = In\frac{r}{R_m} \tag{3.2}$$

Considering a small element in region A, the distance from the element to the center of the tool is r and the thickness of the sheet at the location is t. the strain on the element can be calculated using.

$$\varepsilon_{\varphi}^{A} = \varepsilon_{bending} + \varepsilon_{stretching} \tag{3.3}$$

$$= In\frac{r}{R_m} + In\frac{t_o}{t} \tag{3.4}$$

$$= In\frac{rt_o}{R_m t} \tag{3.5}$$

Where, Rm = tool radius + (t/2) half sheet thickness, the radius of curvature at the middle of the plane of the sheet. R_m = tool radius + (t/2) is only for bending conditions where the tool radius is larger than the sheet thickness.

The strain rate in region A (Figure 3.3) can be determined using equation 3, the element undergoes tensile straining and stresses, if the condition $rt_o/R_m t > 1$ is

satisfied. For the inner surface r =r tool from the above equation, the sheet undergoes maximum compressive bending at this point. The meridian strain is zero when the actual thickness of the sheet satisfies the following condition.

$$t = t^{\varphi} = -r_{tool} + \sqrt{{r_{tool}}^2 + 2r_{tool}t_0} \tag{3.6}$$

If for the deformed sheet thickness t>t□ , the element undergoes compressive stresses and for t<t□, the element undergoes tensile stresses. From (3.7) below the maximum reduction rate on the inner surface which separates the tensile and compressive deformation conditions can be determined.

$$\frac{t}{t_o} = -\frac{r_{tool}}{t_o} + \sqrt{\frac{r_{tool}^2}{t_o^2} + \frac{2r_{tool}}{t_o}} \tag{3.7}$$

For $t/t_o \cong 1$ the zone undergoing compression is small and the thickness reduction ratio is small. The mean strain ε^{-A} for the small element can be calculated using

$$\varepsilon^{-A} = \sqrt{\frac{2}{3}\varepsilon_{ij}\varepsilon_{ij}} = \sqrt{\frac{2}{3}(\varepsilon_t^2 + \varepsilon_\theta^2 + \varepsilon_\varphi^2)} = \frac{2}{\sqrt{3}} In \frac{rt_0}{R_m t} \quad (3.8)$$

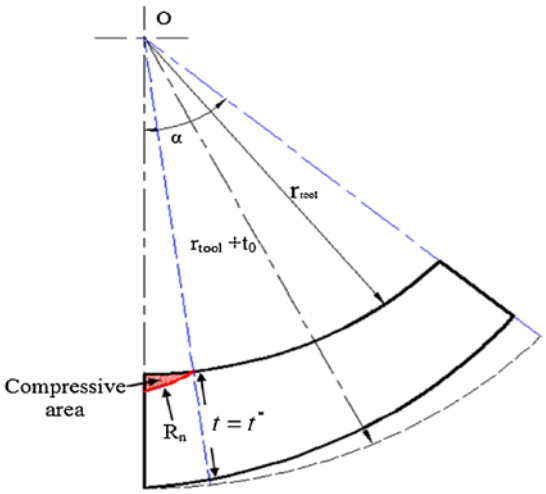

Figure 3.3: Schematic representation of compressive area in ISF process [35]

3.2 Tool Shape

Tool shape has a directly influence on the SPIF process since it determines the area made by the tool and blank in contact. This area has a major influence on the frictional forces acting between the two surfaces. The influence of tool geometry on part formability was investigated by [37]. They used a hemisphere and roller end tool to investigate their effect on formability. They proved that tools with roller end produced parts with higher accuracy than tools with hemispherical ends and that between 5, 10 and 15 mm diameter hemispheric forming tool, 10mm diameter possesses the best formability. [38] Investigated the influence on geometrical accuracy of the shape of the tool. They used hemispherical and flat end tools and found out that flat end tools generally produce parts with higher accuracy than

hemispheric tools. Lower forming forces too are required for flat end tools than round end tools.

[37] Compared sheet formability for flat end tools by varying their lower end radii r and by hemispheric tool having a radius R=5 as shown by Figure 3.4. The radius is kept constant for each tool.

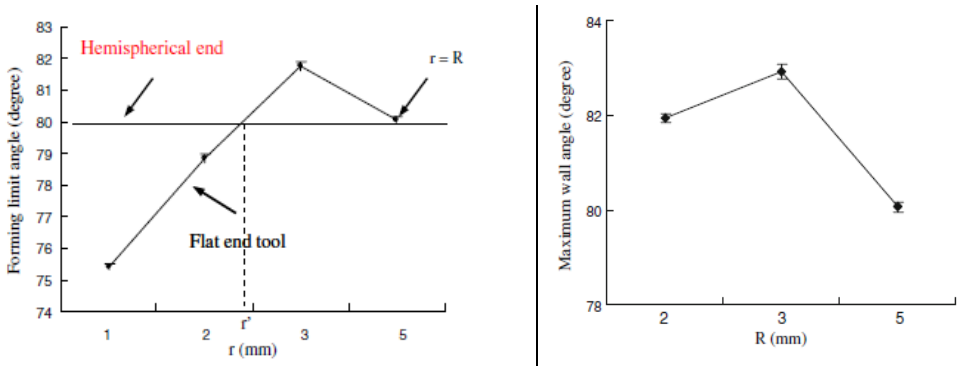

Figure 3.4: The maximum wall angle as a function of the lower end radius of the flat end tool (A). The maximum wall angle as a function of the radius of the hemispherical end tool (B) [37]

As the flat end radius r approaches r there is a general trend. Flat end tools possess lower formability as compared to hemispherical end tools for r < r′ . When the radius r has been exceeded the trend reverses. Formability reduces as r was increased to a certain value r′ (3≤r′ ≤5). Figure 3.4: a) shows that flat tools having radii below 3mm there is a higher formability compared to a hemispherical tool.

From the figure above, formability can be increased using flat tools having the right diameter up to 3mm. Formability also increases to “r” before it starts to reduce. The optimum formability can be determined using 3 ≤ r ≤ 5 for a given sheet. Therefore there is a relationship between the best radius to achieve maximum formability and

the sheet thickness for a given sheet. This is supported by the formability of the round radius R, shown in figure 3.4. [39] Demonstrated that an increase in the radius of the tool leads to a decrease in formability. [38] Proved that for any tool of a given shape, formability is determined by the thickness of the sheet and not the tool radius

3.3 Forming Limit Curves

In SPIF the blank is deformed locally which produces local strains to form a shell work piece. The movement of the tool controls the flow of material unlike in deep drawing process where the flow of material is relatively simple. Failure prediction using conventional techniques such as the stress strain forming diagrams used to determine fracture point in conventional forming processes cannot be applied in SPIF. Forming limit diagrams are very important because they help predict when failure occurs. In traditional sheet forming processes, forming limit curves demonstrate the stress state in the major and minor principal strains. From the plot, necking and failure can be predicted. As shown in 3.5 figure below.

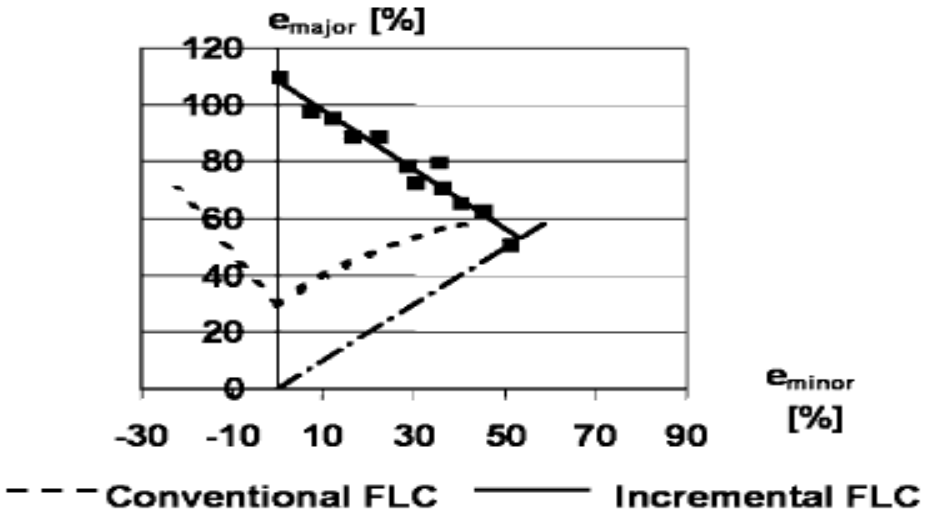

Figure 3.5: Aluminum 1060 forming limit diagram [40]

Formability can be determined using the maximum forming angle, which is a tangent of the deformed sheet to the non deformed sheet. Because of the nature of the application of forces in SPIF, much higher stresses can be achieved without failure compared to traditional manufacturing processes. Therefore conventional forming limit curves cannot be used to predict fracture in SPIF.

In SPIF, a small tool induces high local forces on the blank at the point of contact; these forces are propagated along with the tool as it moves along the blank. This leads to high strains obtained before fracture of the blank. Therefore parts formed by SPIF can typically have longer depths than those formed in conventional processes. The maximum forming angle θ_{max} is an important parameter in determining the type and thickness of a material to be formed in SPIF.

3.4 Crack Propagation

Forming limit curves are usually used in determining how formable a sheet is in the metal forming industry. Unfortunately, the fracture does not follow localized necking in SPIF as demonstrated by [41]. Therefore conventional forming limit diagrams (FLD's) cannot be used to describe failure mode in SPIF.

There are 2 modes of crack propagation as demonstrated in figure 3.6:

• The circumferential "straight" crack propagation path.

• The circumferential "zigzag" crack propagation path.

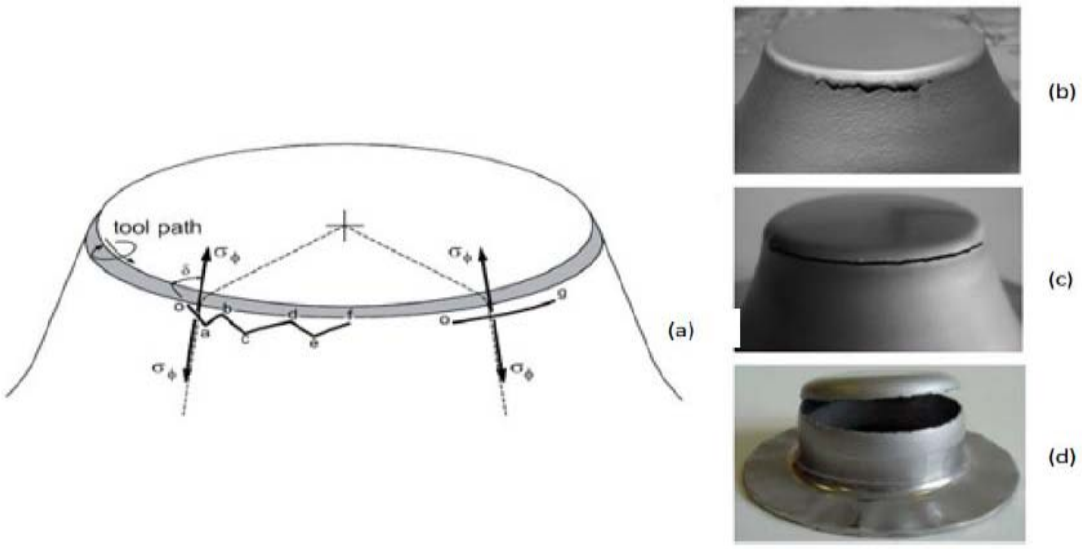

Figure 3.6: Crack propagation in SPIF [42] (a) Scheme of typical propagation path. (b) Circumferential zigzag crack propagation path. (c) Circumferential straight crack propagation path. (d) Circumferential straight crack propagation (part obtained by conventional deep drawing)

The path of the propagation of the crack in fig b (straight along the circumference) is same as that observed in deep drawing and stamping. Circumferential straight crack propagation is caused due by stretching due to σØ. The zigzag crack propagation path (Figure 21 b) is also caused by σØ but the zigzag around the circumferential direction is probably due to friction generated by the forming tool as it rotates. The meridial stresses at the tip of the crack in (Figure a) will be lower than the stresses at the onset point "o". As a result, crack propagation stops and the tool rotates it to point "b" which is similar to the initial point "o", where a new crack starts to form. This mechanism accounts for the typical "zigzag" nature to the crack.

3.5 Formability

Formability is the ability of a metal to undergo plastic deformation without failure. Formability for SPIF can be defined by a range of methods. [42] Used the membrane analysis technique to determine formability. [43, 44] Proposed that formability be calculated using the ultimate angle of incline of the wall, just before failure occurred.

[44] Employed the sine law to predict the minimum thickness of the wall for curved shell parts, and opined that is was the safe thinning limit. Formability for most metals is determined using trial and error tests. [45] Demonstrated that the formability for SPIF is higher than for traditional processes. Formability in SPIF depends on strain hardening, tensile strength and percentage elongation [46]. Many researchers have proposed that high formability in SPIF process is accounted for by material flow behavior. [47] Showed that, for SPIF failure occurs at fracture instead of necking for material undergoing tension.

Major factors that influence formability include radius of the tool, speed of forming and size of step and friction. The interaction between the size of the step and radius of the tool is a major parameter in determining formability.

The step size (vertical) is a very important parameter which determines the time used to deform a blank to the required shape [48]. Large values of step size cause the sheet to stretch and causes premature fracture. Step size should be used taking into consideration the mechanical properties and the blank thickness.

Tool size influences formability of a blank. A larger diameter increases the area of contact between the blank and the tool. Hence deformation is not as a localised as for a small tool. Also more friction is generated between the blank and the tool as compared to a small tool diameter. For this reason, an increasing radius of the forming tool decreases formability. For equal forming depths, larger forming strains are gotten when using a larger forming tool than a smaller one. Therefore tools with small diameter are ideal for forming parts with long depths.

The higher the feed rate in SPIF, the better the formability up to a certain optimal feed rate. A low feed rates the thermal effects due to the friction generated by the motion of the tool and the blank is low and there is no thermal softening of the blank. At higher feed rates, formability improves due to thermal effects. High strain rates induced by very high feed rate can cause early fracture of the blank, as well as a sudden rise in temperature in the surrounding parts of the blank. This decreases the resistance to deformation and leads to early fracture.

The effects of temperature in SPIF on formability (maximum forming angle) have been studied by (49) for composites and they came to the conclusion that formability increases to a certain optimal value of temperature before it starts decreasing.

3.6 Tool Path

Besides other parameters that affect SPIF such as tool radius, feed rate and processing speed, tool path trajectory has a major role in formability and accuracy. In SPIF adjustments in geometry can be easily done, therefore generation of tool path becomes a key point linked to SPIF. The tool path is particularly important because it directly determines part accuracy and key variables like processing time, quality of the surface, thickness variation and formability.

Part accuracy is a major drawback affecting industrial use of SPIF. Although most parts produced on industry require a dimensional accuracy of ±0.5mm, most parts produced by SPIF have more dimensional inaccuracy [50]. Shape and dimensional inaccuracies in SPIF have been shown by [51] and they employed several strategies to overcome them including multipoint and back draw incremental forming, the use of flexible support, optimised trajectories and counter pressure.

[52] Demonstrated that, improved accuracy is gotten by running the tool from the edge to the centre of a blank in SPIF. [53] Tested two tool path types and came to the conclusion that spiral tool path are better than contour tool paths because it eliminates scarring resulting from step downs in the tool path z-level contouring.

[54] Experimented on the influence of axial increment on metal forming and proposed that little scallop heights and changing axial increments can be used to determine the best tool path.[55] Used a CAD model with a higher slope angle to compensate for the spring back effect. [56] Named this 'vitiated trajectories' since the tool path is falsified deliberately to form accurate parts. [55] Showed that a multi step tool path approach can allow for low forming stresses, especially at the wall, this increased the accuracy of the formed part.

Determination of tool motion is highly developed for milling processes, although the mechanism not same as what occurs in SPIF, the equipment and motion control are same. Therefore integrating process parameters such as machine dynamics and using NC programs in controlling tool motions and simulations can improve results in the SPIF.

There exist no specific tool paths that best suits the SPIF process [55]. Proposed Intelligent Computer Aided Manufacturing (ICAM) which uses real time process data to evaluate and control the movement of a tool. This is done using CAD-CAM interference using specific process parameters. The ICAM model (see Figure 3.7) has been successfully used to produce many part of consistent wall thickness and can easily be applied in industry.

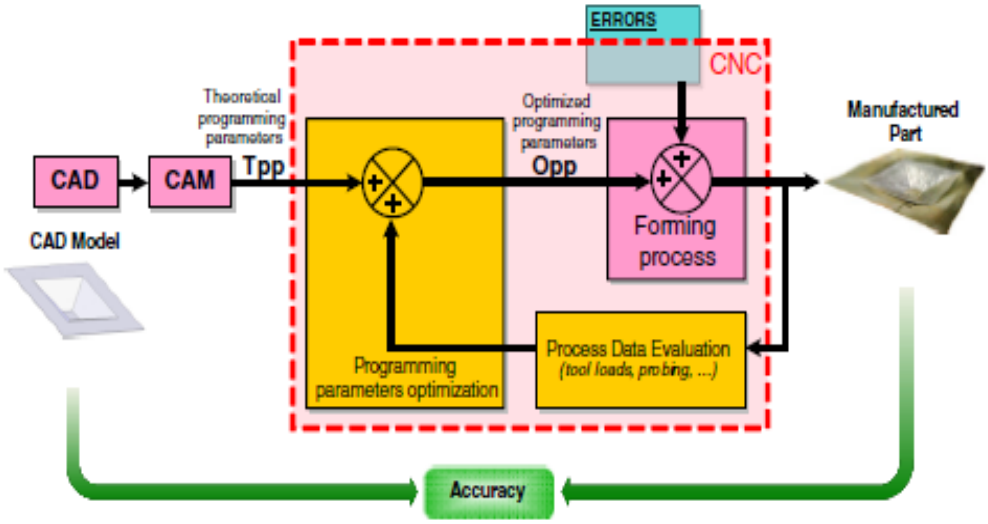

Figure 3.7: Using ICAM approach to manufacture a part from the CAD model [55]

3.7 Forming Angle

The forming angle is the angle between the formed wall and the horizontal part of the blank. The forming angle is dependent on the property of the material and blank thickness. Formability is determined in SPIF by defining the highest angle (θ_{max}) of deformation a blank can withstand in the absence of failure during a single pass. [57] Attempted to predicting the maximum forming angle through the use of forming parameters and material properties and shown in (3.9).

$$\psi = \frac{\pi}{2} - \left(\frac{\sigma_Y}{\sigma_\emptyset} - 1\right)\frac{r_{tool}}{kt_o} = \frac{\pi}{2} - \left(\frac{kt}{r_{tool}}\right)\frac{r_{tool}}{kt_o} = \frac{\pi}{2} - exp^{\varepsilon_t} \quad (3.9)$$

In which:

t= fracture thickness at forming limit, ε_t= thickness fracture limit stain.

This equation can be used to determine the onset of fracture since ideas of fracture at the limit of formability in principal strain direction and the angle just before failure can be determined. The above equation can be expressed using the sine law demonstrated in Figure 3.8.

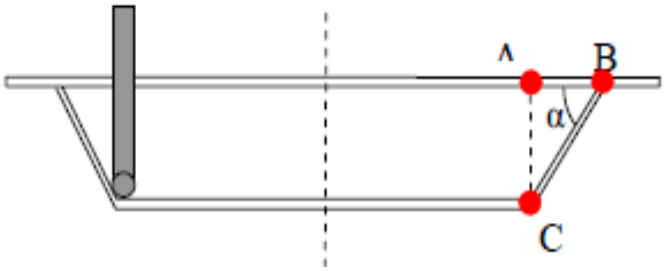

Figure3.8: Sine law showing the maximum forming angle [57]

$T_{BC} = T_{AB} \text{ Sin } (90-\alpha)$ (3.10)

In which:

T_{BC} = thickness of the deformed sheet.

T_{AB} = thickness of the non deformed sheet.

A steeper wall angle leads to greater thinning in the zone BC zone as shown by equation. The maximum wall angle before failure is improved through adding the blank's initial thickness T_{AB} but this leads to increased force requirement for deformation which may be more than the machine load. Also more thickness may not meet design specifications.

Higher wall angles can be obtained by using multiple tool passes to progressively deform the blank to the required specification. This reduces the stresses required, however forming time increases considerably.

3.8 Step Size

The role of step size in SPIF and its influence on formability is not well understood. Some researchers are of the opinion that step size only influences surface roughness and not formability while others are of the opinion that it influences formability, a higher step size decreases formability. [58] Proved in a study that step size significantly influences formability. Step size has been proven to affect outer and

inner roughness of surfaces and also the forming time. Increasing small steps along the z-plane demand more time in forming due to part specifications. Roughness tends to be dependent on the forming angle and the tool size.

3.9 Forming Speeds

Generally an increase in forming speed increases formability because the heat generated heats the surrounding metal and 'softens' the metal which as a result requires less forming forces hence improved formability. The feed rate during incremental forming is a summation of the tool's rotational motion and the tool's feed speed. Increasing the rotation of the tool increases roughness of formed parts. Using higher forming speeds, lead to an increase in the heat generated and the coefficient of friction between the blank and the tool, since friction between the tool and blank is directly proportional to the relative motion between them. An increase in the feed speed of the tool does not significantly affect the formability; however it decreases the final forming depth.

Other effects of high feed rate on SPIF include increased sheet waviness, tool wear increases, breakdown of the lubricant film and increased marks on the blank resulting from tool chatter.

3.10 Lubrication

Due to friction generated from the contact between the blank and tool, proper lubrication is needed to improve surface quality and reduce wear of the tool. Although tool wear is minimal at low temperatures, it increases significantly at higher temperatures and may lead to errors in specifications of parts to be manufactured may not be met. At high temperatures the blank material becomes

‘soft’ and can be easily distorted at the surface. Lubrication improves the surface quality by reducing this effect.

Sliding friction which is generated by the effective tool speed should be minimized by reducing the feed speed to avoid tearing of the sheet. Therefore proper lubrication of the blank is required to achieve large forming depths. [38] Showed that large contact forces squeezes out organic lubricants, greases, oil form the blank-tool contact and proposed that inorganic lubricant (98.5% pure MoS2 powder with medium grain size) mixed with grease be used and with an iodized sheet.

Chapter 4

RESEARCH METHODOLOGY

In this section the experimental techniques are described. The tools, experimental conditions and the reasons for selecting the experimental material, aluminium 1060 (commercial aluminium) are given.

4.1 Material Properties of Aluminium 1060

During the experiment commercial aluminium (1060) was used of sheet thicknesses 1mm and 1.5mm. The sheets were cut from the initial stock of 1mm by 3mm using a guillotine. The dimensions of the work sheets have specification 160mm x 160mm. However, the working area has length 100mm and width 100mm at the centre. The remaining area is used for clamping the sheet in place. The mechanical properties of the sheets are unknown and cold/hot working during the manufacturing process may have influenced the mechanical properties of the sheets.

Cold working (sheet rolling) during sheet manufacturing causes points of defects and energy being stored in dislocations. During annealing there is a huge reduction in dislocation points and defects along the grain boundaries. Annealing also eliminates directional properties in the material, increases formability and makes for more accurate results from the tests. Annealing (homogenisation) is popular before cold working to obtain fine and homogenous structure that can guarantee good forming responses in manufacturing operations. The fine grains generated lead to improved ductility and hence formability.

A study carried by [59] proved that annealing aluminium sheets by heating for 8hours in an oven at 430^{o}C is cost effective and efficient. The temperature in the oven is first raised to a temperature of 430^{o}C; the sheets are then placed there and closed. After the time period the sheets are placed in the surround environment and allowed to cool.

Samples from the annealed sheets were cut using a CNC machine and the mechanical properties were determined using tensile tests using A370-09 standards. The samples were of the following geometric specifications: guage thickness 1mm, 28mm length and 6.25 width as shown in figure 4.1.

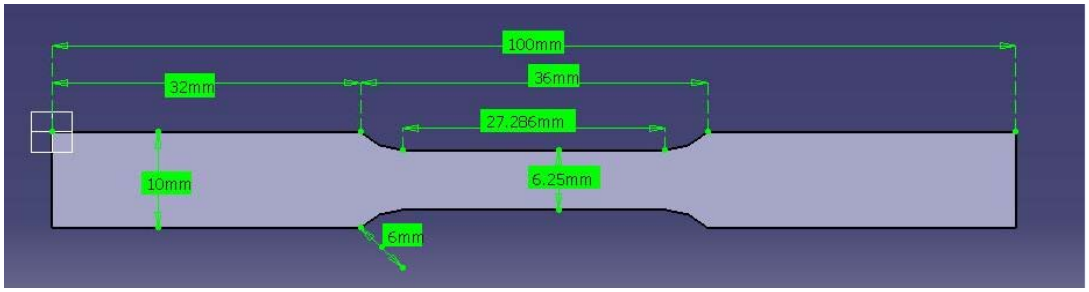

Figure4.1: Dimensional specifications for tensile samples

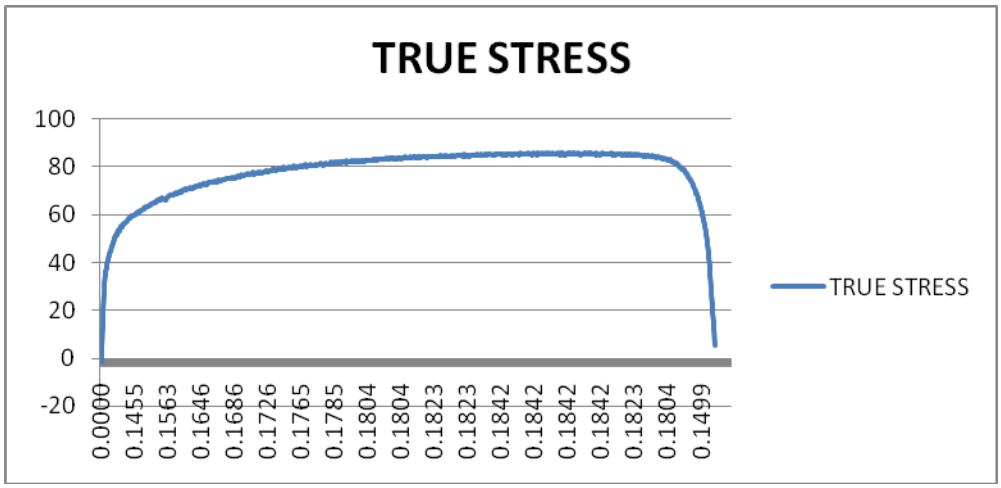

Figure 4.2: stress strain curve of true stress and strain

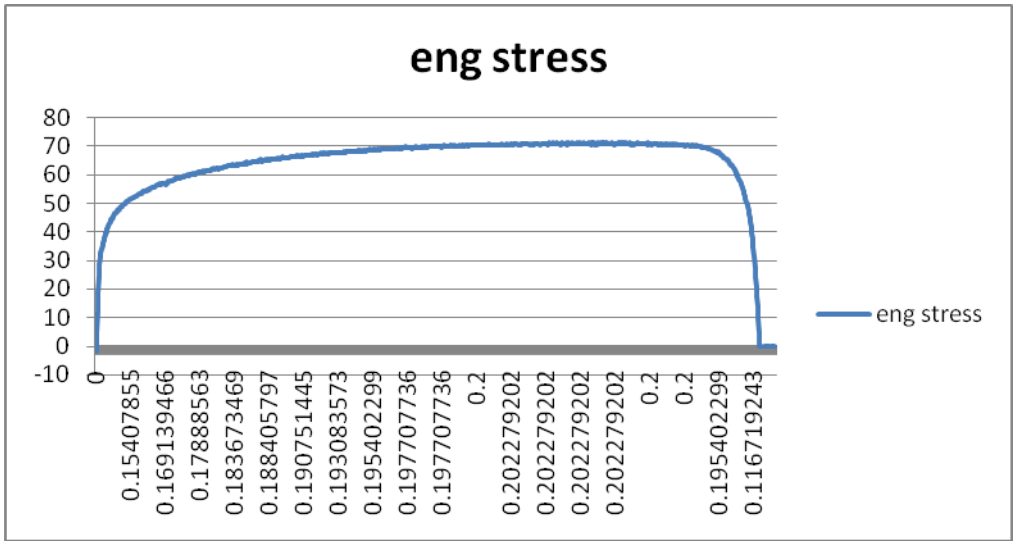

Figure 4.3: Engineering stress and strain curve

The stress-strain data (Figure 4.2 and 4.3) were obtained from experiments performed in the Middle East Technical University material science lab on samples of the annealed material. The complete data is provided in the appendix. The mechanical properties of the annealed sheets are given below.

Table 4.1: Material properties of aluminium 1060 annealed

	Unit	**Symbols**	**Value**
Density	MPa	Kgm^{-2}	2710
Young modulus (modulus of elasticity)	G	MPa	72000
Poisons ratio	E	MPa	0.33

Al1060 was selected as the working material for this research because of its availability and cost. It has excellent formability using commercial techniques both for cold and hot working; it can be welded and is corrosion resistant. However, it has low strength similar to pure aluminium. The chemical composition of aluminium 1060 is provided in the table below.

Table 4.2: Chemical compositions of Al1060 sheets (mass fraction,%)

Si	Fe	Cu	Mn	Mg	Ni	Zn	Ti	Al
0.20	0.25	0.06	0.02	0.018	< 0.01	0.055	0.014	Bal.

To obtain the final shape for the deformed sheet the part is modelled in CATIA V5R. The part design is then imported to a CAM software POWER MILL 5. Points along the desired profile are obtained.

The data can then be sent to the CNC milling machine for machining or converted to an INP file and imported as coordinates for F.E.A simulation. The analysis is designed to optimise the bulge height given the equipment and material. This is done by using a slope angle of 65^0.

The results are obtained using.

- Single point incremental forming on the CNC machine tool.
- Finite element analysis on Abaqus (6.12).

A strong correlation between the results obtained from practical work and F.E.A would justify the results and serve as an explanation for pillow formation.

4.2 Experimental Set Up

The experiment is presented in the following subsections: CNC machine tool, forming tool, lubrication, clamps and tools used during the procedure.

4.2.1 The CNC Machine Tool

The experiments were carried out in CAD/CAM laboratory of the department of Mechanical Engineering, Eastern Mediterranean University. We used a Dugard ECO 760 Vertical Machining Centre with specifications on table 4.4.

Table 4.3: Technical specifications of machine tool

Technical specifications of machine tool	
Operating system of CNC	Fanuc OiMD
Number of axis of freedom	3
Machine capacity (maximum travel in x,y,z in mm)	760, 430, 460
Maximum tool diameter (mm)	100mm

4.2.2 Forming Tools

The tools used to deform the sheets are held with a tool holder. The movement of the tool is controlled using G codes input into the CNC milling machine. The tools are made of high speed steels and have diameters 10, 14 and 20mm. One of the 10mm diameter tool is round while the other tool is flat with a small chamfer. The difference in tool geometry is used to examine its effect on pillow formation (part accuracy). In the experiments different tools are used to form the sheets in order to check the result of variations on tool geometry and radius during pillow formation taking into consideration sheet thickness. The pictures of the tools are shown in Figure 4.4 below.

A B

Figure 4.4: (A) Round end tools with diameters and 10,14 and 20mm. (B) Flat end tools with 10 and 14mm.

The experimental plan is laid out in the table 5.4 below to be used to determine the effect of each parameter on the outcome of the results.

Table 4.4: Showing the process variables

Tool diameter (mm)	Tool geometry	Sheet thickness (mm)
10	Round	1
10	Flat	1.5
14	Round	1.5
14	Flat	1.5
20	Round	1.5

4.2.3 Clamping System

The SPIF experiments were performed with the help of the clamping system shown below in Figure 4.5.

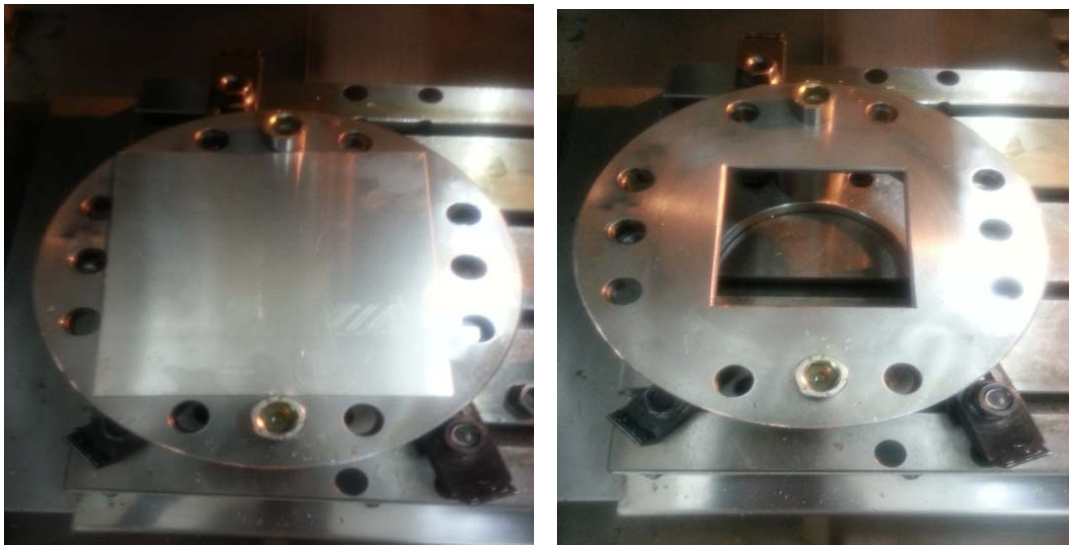

A B

Figure 4.5: (A) Back plate with the blank on it. (B) Clamping system used showing the back plate

The jig is made up of a circular down frame fixed to the machine table with the help of 14mm diameter screws. Four bars are used to raise the blank holder from the machine table to provide room for the formed sheet. A circular blank holder is used to fasten the sheet on a square back plate. They are fastened on the circular frame. The working area of the pyramid is 10000mm^2 (100mm X 100mm).

Care must be taken when assigning coordinates for the movement of the tool to prevent collision between the blank holder and the tool because this would lead to damage of the sheet. The edge of the square back plate is chamfered to prevent early failure (necking of the sheet) as it is formed to due induced stresses.

Lubrication is very important in SPIF because it reduces wearing and improves the surface quality. During the experiments grease is used as the lubricant. The feed rate is kept at 500mms^{-1} throughout the experiments. The tool is held firm and is not allowed to rotate during the experiments. Figure 4.6 and 4.7 show the process in operation and at the end of the process.

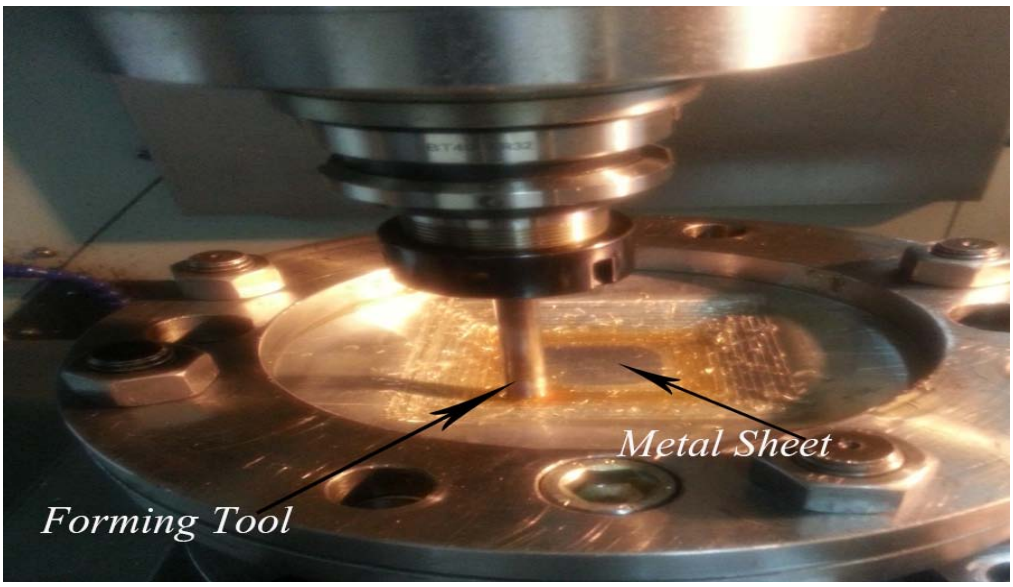

Figure 4.6: Incremental Forming Process in Progress

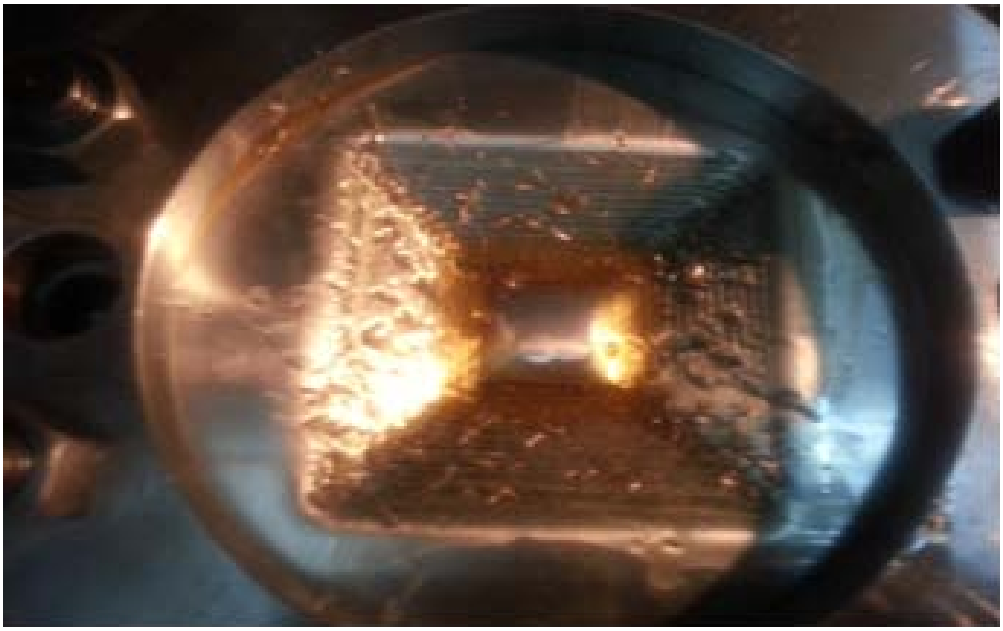

Figure 4.7: SPIF in progress (sharp edge of the tool causes chips)

4.3 Finite Element Analysis of the Incremental Forming Process

Simulations are essential to understand physical processes as they can be modelled as partial or integral differential equations. The finite element method was first used to simulate elastic-plastic applications by [60] and since then sheet forming operations like stamping, hydro forming, incremental forming, etc have been modelled in order to better understand the forming processes, defect prediction and forming parameters. Finite element analysis (FEA) can be utilised to investigate the influence of operation parameters in SPIF. Implicit (Langrangian formulation) model or the explicit model can be used to simulate. Explicit FEA has been shown to be a cost effective (computational time) and close to the real experiments for simulating SPIF process [61].

Finite element analysis of the process was done with ABAQUS 6.12-1. The software is less costly in terms of computing power needed and time needed to simulate the

process because it has the option of elastic-plastic behaviour and rigid-plastic deformation. This reduces the time needed to design the parts in the simulation.

One of the most difficult aspects of simulating SPIF is the definition of tool path because tool path definitions in FEA softwares typically need to be programmed in some other programme and imported to the FEA software. The tool path can be defined in ABAQUS by using point to point (displacement rotation, velocity angular velocity acceleration angular acceleration). In this study the tool path is defined using tool displacement. An amplitude is used to define the variation of forces during the process. Equally spaced amplitude is used to define the tool displacement.

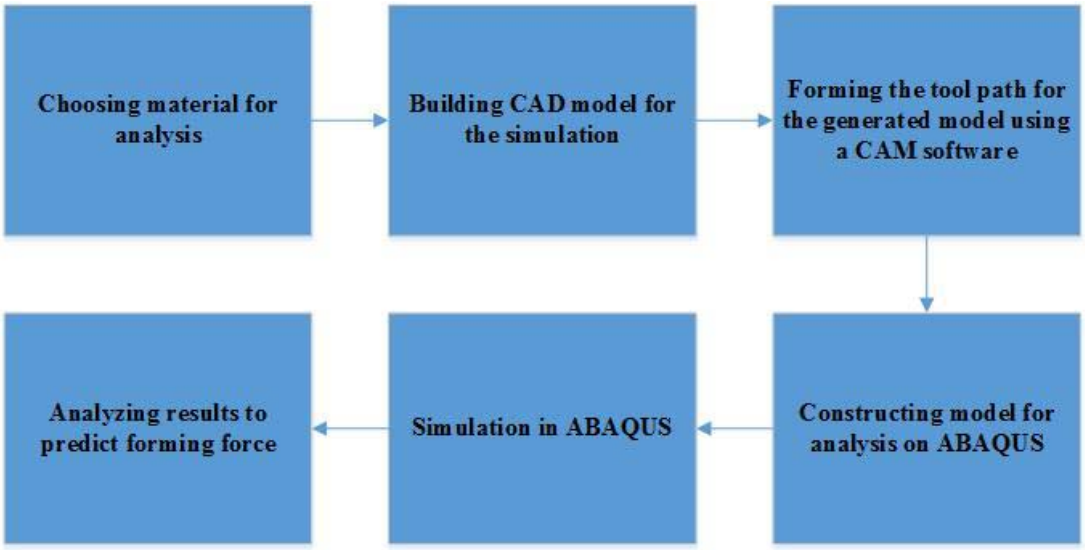

Figure 4.8: Steps in FEA simulation of incremental forming

In the pre-process (before simulation), the 3D geometry to be obtained is drawn using a CAD (CATIA) software. This 3D geometry is imported to a CAM (NX 9) software. Here G codes are assigned to a tool developed in the software, which is used to create x,y,z amplitude along the profile of the drawn part to be obtained. This software produces a CL (cutter location) file from the G codes. These points are

imported to TOOL PATH GENERATION software. This is fed into ABAQUS as an amplitude definition (INP File).

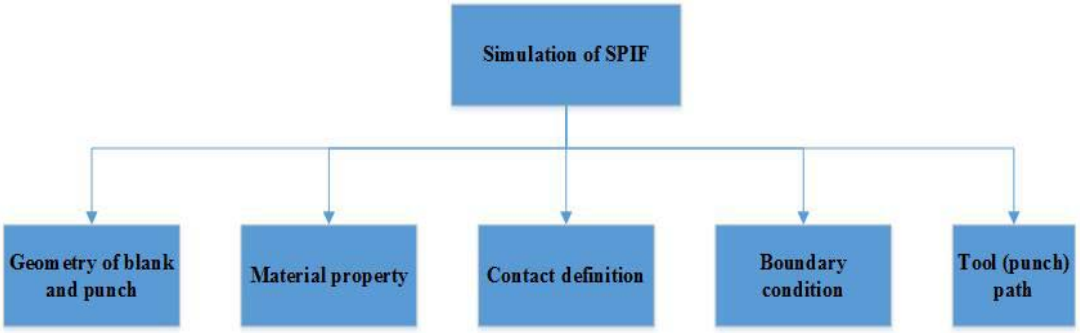

Figure 4.9: Steps in building the FEA model on ABAQUS

The tool and blank geometries are defined. The blank is a 3D deformable homogenous solid. The tool is a revolved 3D analytical rigid element. In the section assignment, the material properties of Al1060 (see Figure 4.10) are assigned to the Aluminium blank.

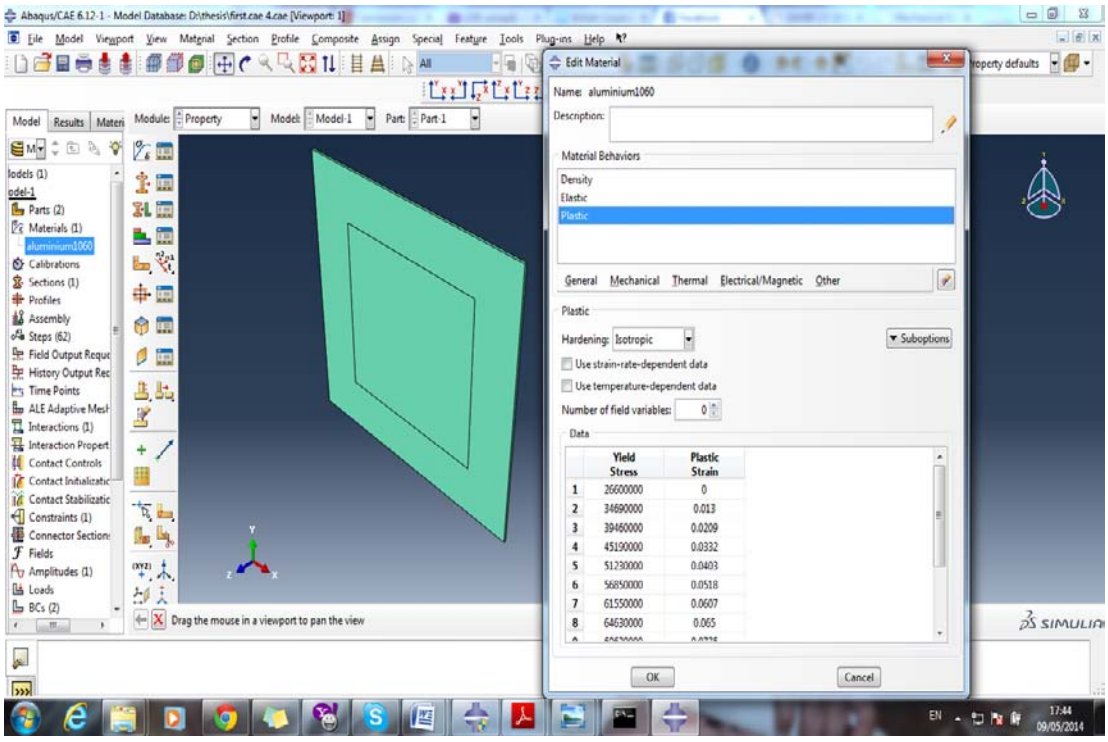

Figure 4.10: Assigning material properties to blank

The blank is then meshed as in Figure 4.11. Mesh size is a very important parameter since smaller mesh increases the accuracy of the results, on the other hand this increases the simulation time. In this study a mesh size of 1mm is used. In FEA soft ware rigid surfaces cannot be meshed nor a material property assigned as they are basically used to simplify an interaction where there is little or no deformation of the rigid surface. The rigid surface here is the steel tool because it is harder than the aluminium sheet.

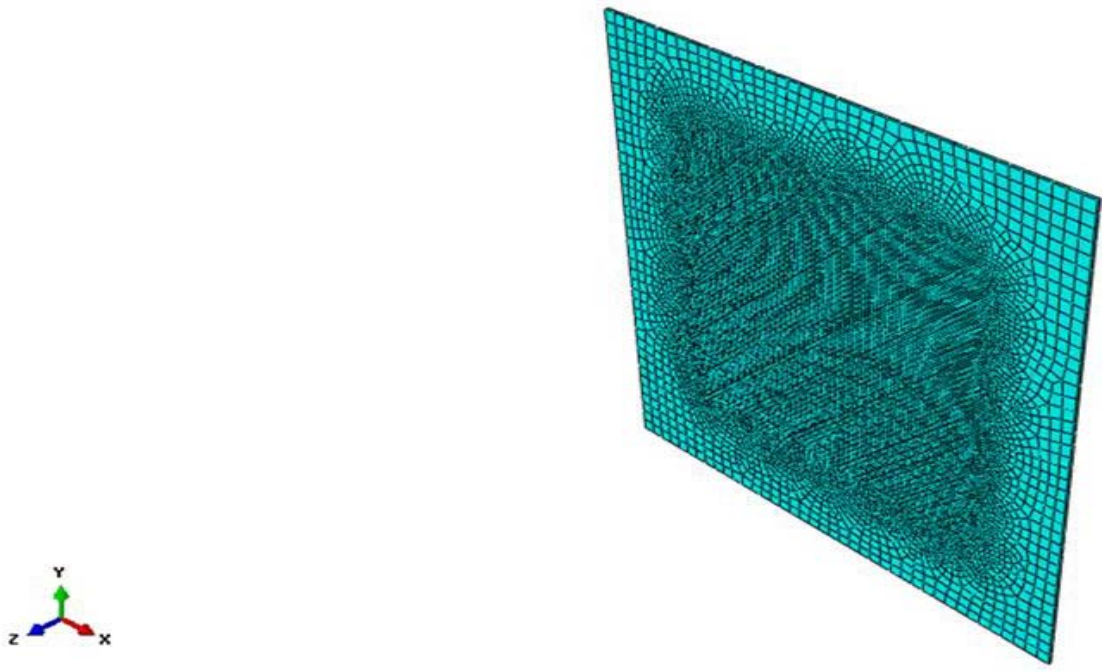

Figure 4.11: Meshed assembly

The contact property is selected as normal contact and a coefficient of friction of 0.1 is assigned (using contact penalty). This is due to good lubrication during the SPIF. The interaction condition is chosen as all shell. In order to get good results the edge of the flat tool in contact with the sheet has a fillet of 1 radius. This reduces the tendency of the tool to distort the mesh in the blank. Based on prior research made by [62] C3D8I mesh performs better than other mesh types (C3D8R and CD38) in

incrementally formed parts. Therefore this mesh was type opted for in F.E.A modelling of single point incremental forming.

The stimulation is simplified with the use of boundary conditions to stop the blank instead of the clamps as it done for the experiments; this reduces the computational time and the possible errors. The steps in the simulation are indicated.

The blank is held fixed at the area where there is interaction with the clamp with the used of boundary condition encastre, which stops all the 6 degrees of freedom of motion at the boundary points, while the movement of the tool is defined along the 6 degrees of freedom using a velocity boundary condition. The amplitude of the force applied is defined for each step during the simulation. The displacement and time of the tool motion are inputted into the steps. The boundary conditions are shown in figure 4.12 below.

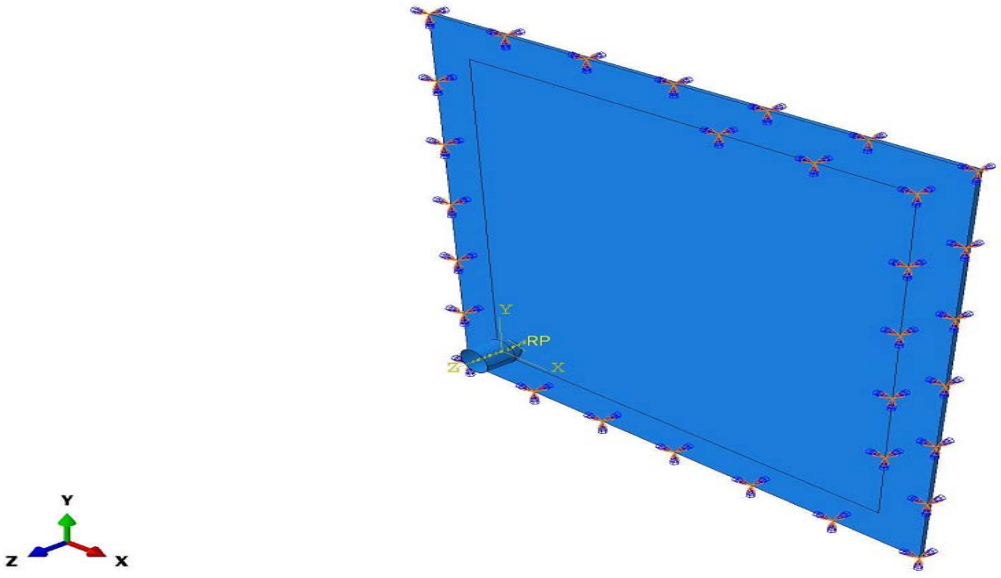

Figure 4.12: Boundary conditions for the tool and blank during analysis

The job is submitted for analysis as a dynamic explicit simulation. Figure 4.13 below shows the job at the beginning and 4.14 shows the job at completion. Analysis of each model takes approximately 8 hours. From the output data base we can extract information regarding stress, strain, displacement, temperature, etc at different time frames for different steps in the simulation. We can also obtain information for specific areas, surfaces and nodes. Through the information obtained, relevant insides can be determined which would help us better understand SPIF.

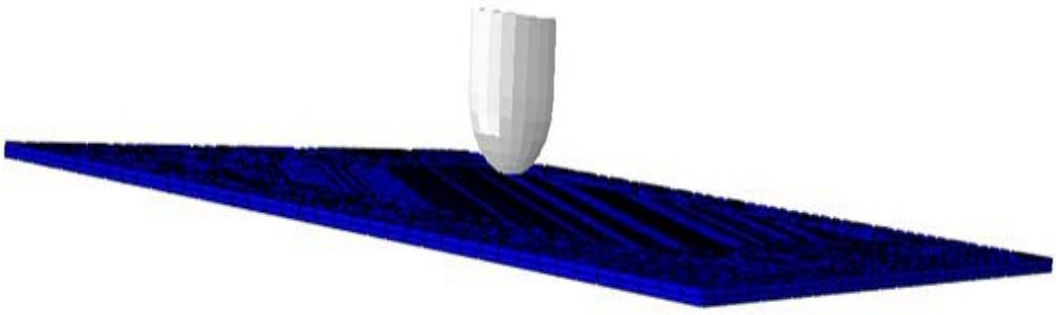

Figure 4.13: Non deformed blank at the beginning of the process

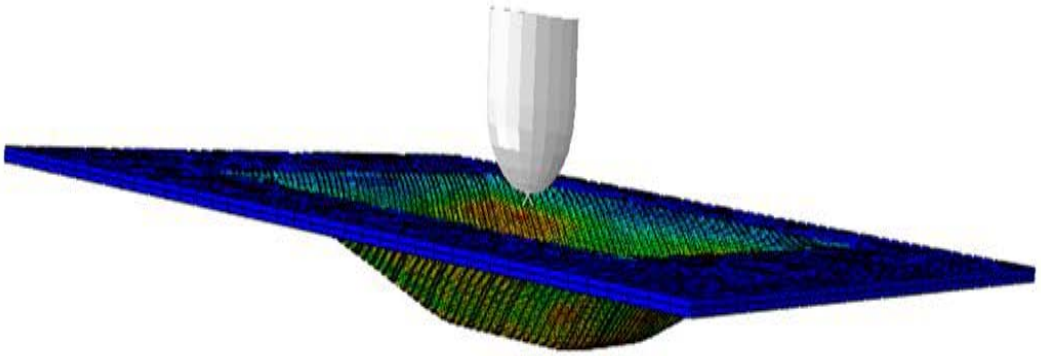

Figure 4.14: Deformed blank at the end of the process

Chapter 5

RESULTS AND DISCUSSION

The effects of the tool size, tool shape and sheet thickness on pillow height are discoursed in this section. In an effort to understand what causes pillow formation, the thickness along the profile is measured to check the material behaviour during the process. The obtained pillows are compared with the stimulation results to compare trends in on process parameters. The stress states are examined for one of the experiment (simulation) for the bottom and top surface to observe variations in stresses and attempt an explanation for the pillowing mechanism.

5.1 Measurement of Pillow Height

The pillow heights are measured using a digital venire calliper with an accuracy of 0.01mm. The measurements are made from the base of the specimen to the maximum pillow height at the centre of the blank.

5.2 Effects of Process Parameters on Pillow Height

In this section we would be investigating the effects tool shape, tool size (tool radius) and sheet thickness on pillow height. This would serve as a guideline in determining how pillow formation can be minimised.

5.2.1 Effect of Tool Shape on Pillow Height

The effect of tool geometry on pillow height is investigated using 10 and 14mm round and flat tools. It is observed that the pillow height is higher for the round tool than for the flat tool. Also the height decreases with an increase in the tool diameter.

Table 6.1 below shows the pillow height due to forming using 10 and 14mm diameter flat and round tools with a sheet thickness of 1.5mm. It should be noted that the pillow heights are taken at a forming depth of 12mm. Figure 5.1 demonstrates the practical and F.E.A results.

Table 5.1: Effect of tool geometry on pillow height

Tool geometry and size	Maximum pillow height (mm)
10 mm flat	1.5
10 mm round	2.17
14mm flat	0.7
14mm round	1.81

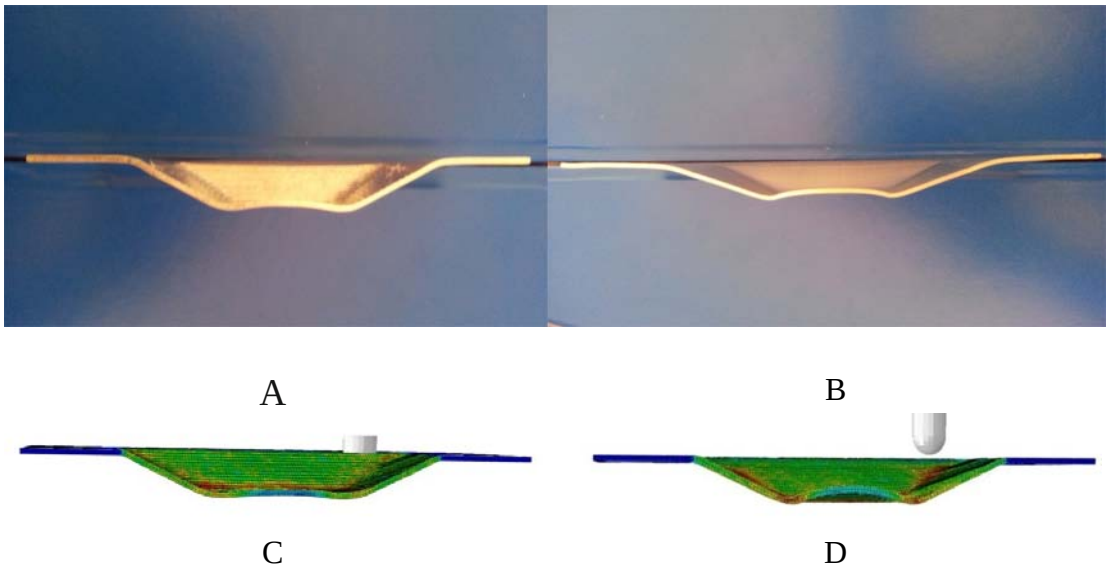

Figure 5.1: (A, C).Effect of 10mm flat tool on pillow height practical and FEA. (B, D) Effect of 10round round tool on pillow height practical and FEA.

5.2.2 Effect of Tool Size on Pillow Height

An increase in the tool size (tool radius) leads to reduction in the pillow effect. This is shown in table 5.2 below and represented in 5.2.

Table 5.2: Effect of tool size on pillow height

Tool radius	Maximum pillow height mm
10mm round	2.17
14mm round	1.81
20mm round	1.3

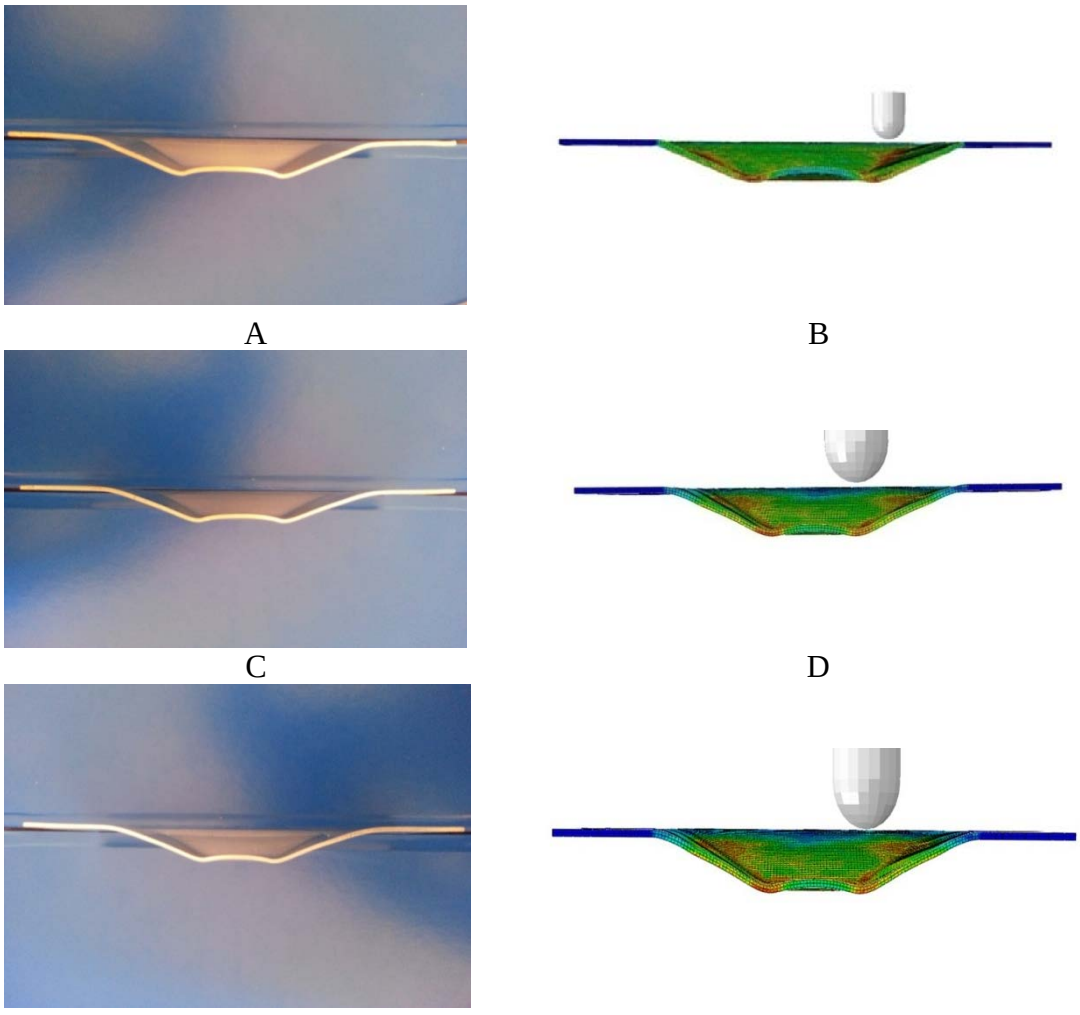

A B C D E F

Figure 5.2: (A, B) Effect of tool diameter on pillow height 10mm round tool.(C, D) Effect of tool diameter on pillow height 14mm round tool. (E, F)Effect of tool diameter on pillow height 20mm round tool

5.2.3 Effect of Sheet Thickness on Pillow Height

An increase in the sheet thickness leads to an increase in the pillow height for same tool. This is shown on table 5.3 and figure 5.3 below.

Table 5.3: Effect of sheet thickness on pillow height

Tool diameter (1mm)	1 mm sheet thickness	1.5mm sheet thickness
Maximum pillow height (mm)	1.72	2.17

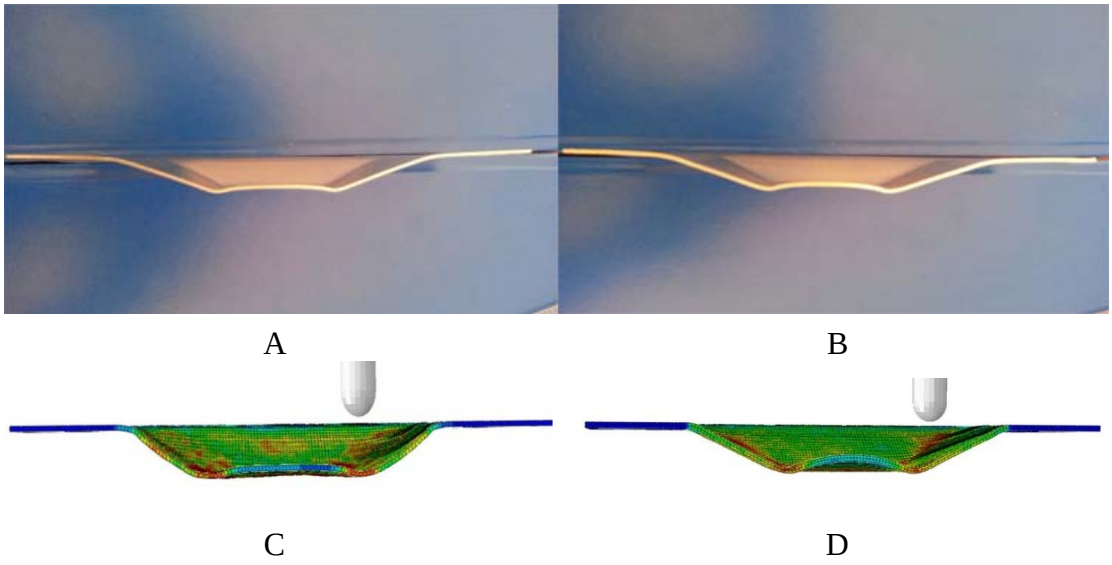

A B

C D

Figure 5.3: (A, C) Effect of10mm round tool and 1mm thick sheet. (B, D) Effect of 10mm round tool and 1.5mm thick sheet

5.3 Thickness Measurement Along the Profile

The sheet thickness is measured using an electronic venire calliper along the cut profile to check variation in the thickness. Understanding thickness of the blank would serve to better control pillow formation, since areas of increased thickness may be due to material flow or blocking of the material.

Figure 5.4: Measuring the variation in sheet thickness along profile of the sheet

From the readings taken for the profile see Figure 5.4, it is observed that there is a reduction in the sheet thickness form the original blank thickness as the depth increases. The thickness is minimum just before the bottom of the formed part. Thickness then increases slightly as at the bottom. The thickness at the middle of the wall is same as the value predicted by the sine law for the said angle.

There is an increase in thickness at the point of contact of the tool and the bottom of the formed part. This part becomes thicker than the original blank thickness. The thickness however reduces towards the centre of the blank.

5.4 Stress and Strain States Along Cut Profile and Pillowing Mechanism

The stress state along the cut profile can be determined using the output data base of the FEA results. From these results we could get some insights into understanding and controlling the formation of the pillow**.** Block elements were used for simulations in FEA in and stresses corresponding to various axis of motion can be considered.

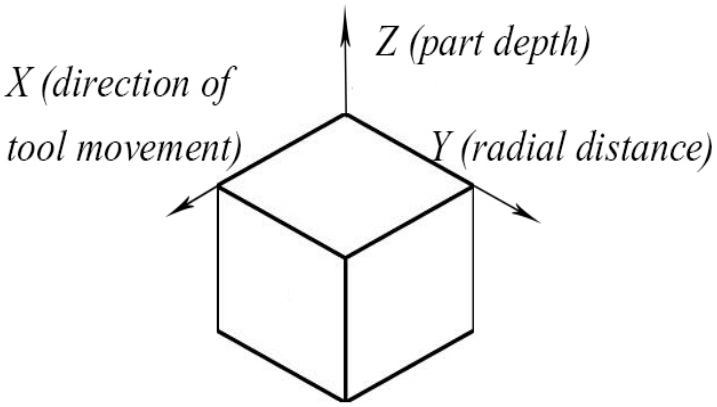

Figure 5.5: Block indicating the directions

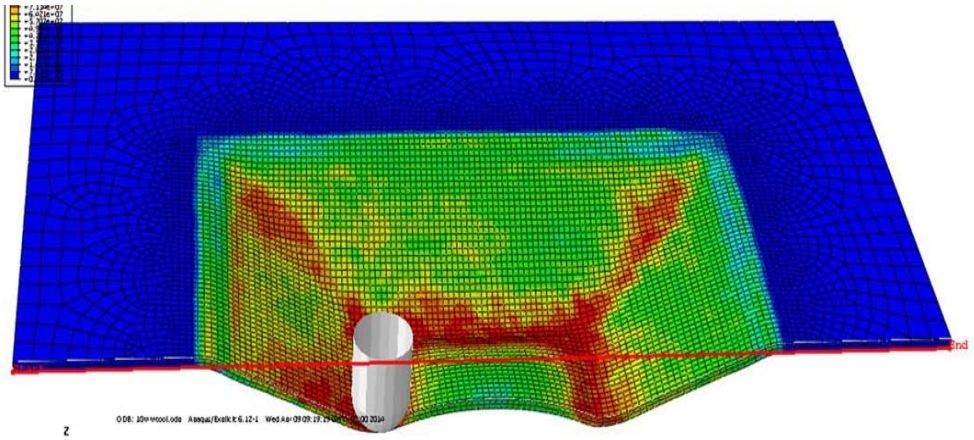

Figure 5.6: Profile through which stresses and strains were determined at a depth of 11mm with the forming tool in contact with the blank

The stresses on each element can be determined at any step during the simulation to obtain valuable information on the stress and strain state of the element. By defining a line on the top and bottom surfaces of the elements we can determine the nature of stresses forces acting on the body (Figure 5.6). Positive stresses on a phase of a body are considered as tensile while negative forces are considered as compressive. An example to illustrate how stresses are determined is explained below.

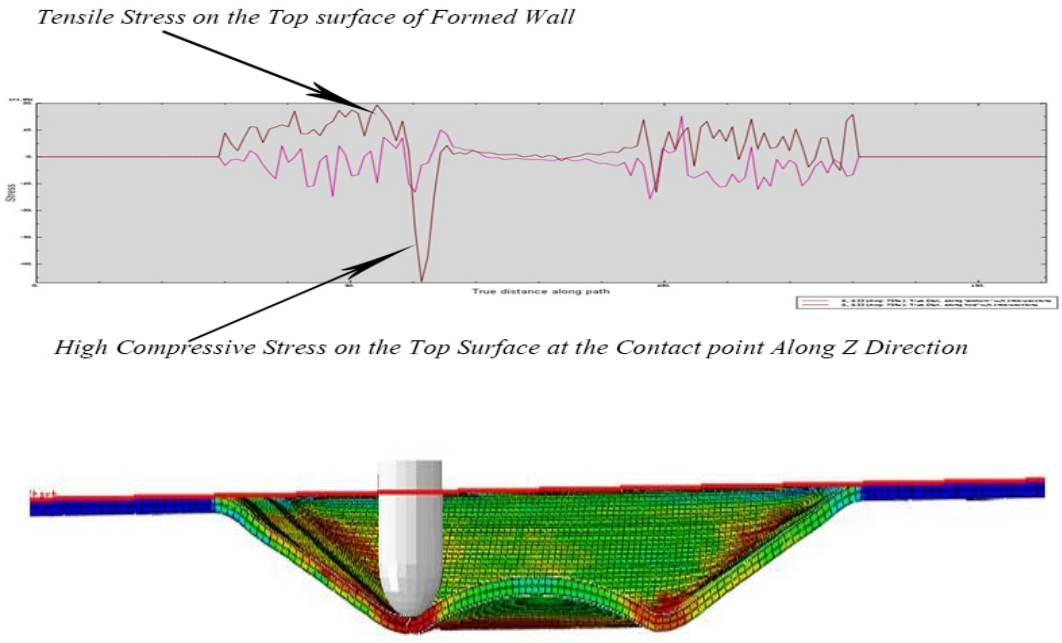

Figure 5.7: Demonstrating stress state along cut profile

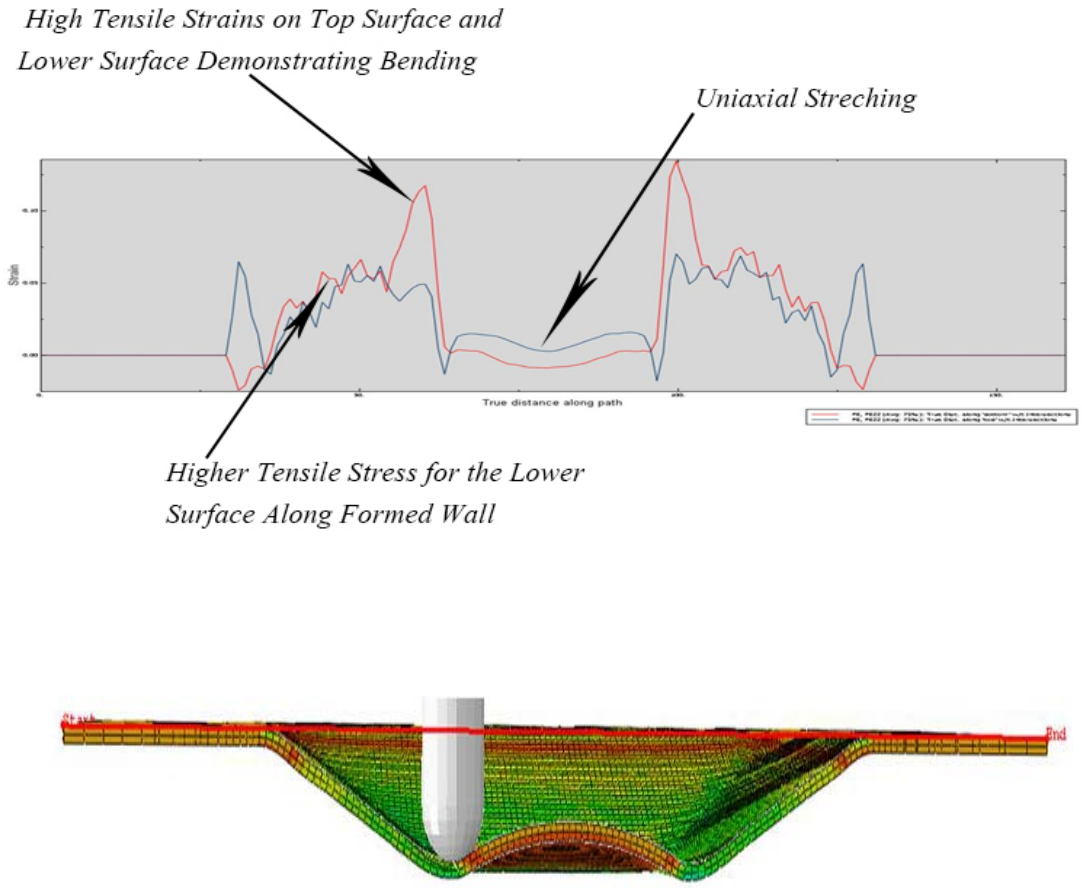

Figure 5.8: Demonstrating strain state along cut profile

Bending can be determined form the strain results when there are forces with same signs but same or different magnitudes acting on the body at a point along the defined line. To determine zones undergoing stretching forces act on the surfaces in opposite directions.

The series of diagrams below show the stress and strain states for the parts at a forming depth of 12mm with the tool in contact with the part.

At the point of contact of the tool, in the Z direction, compressive stresses on the top surface of the sheet are greater than those on the bottom surface due to the forces induced by the tool on the upper surface of the sheet at the point of contact. This offsets the neutral axis along the plane of sheet and causes severe bending under tension. This squeezes the elements of the blank on the top surface causing them to have more negative strains compared to the lower elements. Hence the top elements are more compressed in the Z direction than the lower elements.

Along the y direction, tensile forces act on both the top and bottom surfaces. The elements are elongated in this direction. It is demonstrated by tensile strains in this direction being positive.

In the x direction, the direction of tool movement, there are compressive stresses acting on both surfaces of the blank. The magnitude is higher for the top surface due to higher forces caused by the tool motion. This causes compression of elements along the top surface and expansion of elements in the bottom surface, as shown by the strain curve at the point of contact.

Towards the centre of the part, stresses along the Z direction tend towards zero for both the top and bottom of the sheet. However, in the Y direction (radial direction) there is a significant difference in stress values for the top and bottom surface. The top surface undergoes tensional stresses while the bottom surface undergoes compressive forces. This is due to transmission of forces induced by the tool on the part at the point of contact between the tool and blank.

S22 stands for stresses along the direction perpendicular to the tool movement (Y). S33 stands for stresses along the direction of the depth of the formed part (Z).

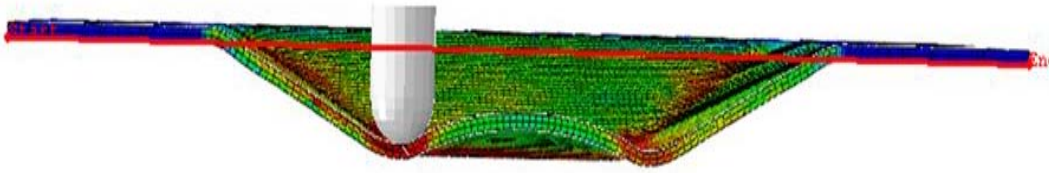

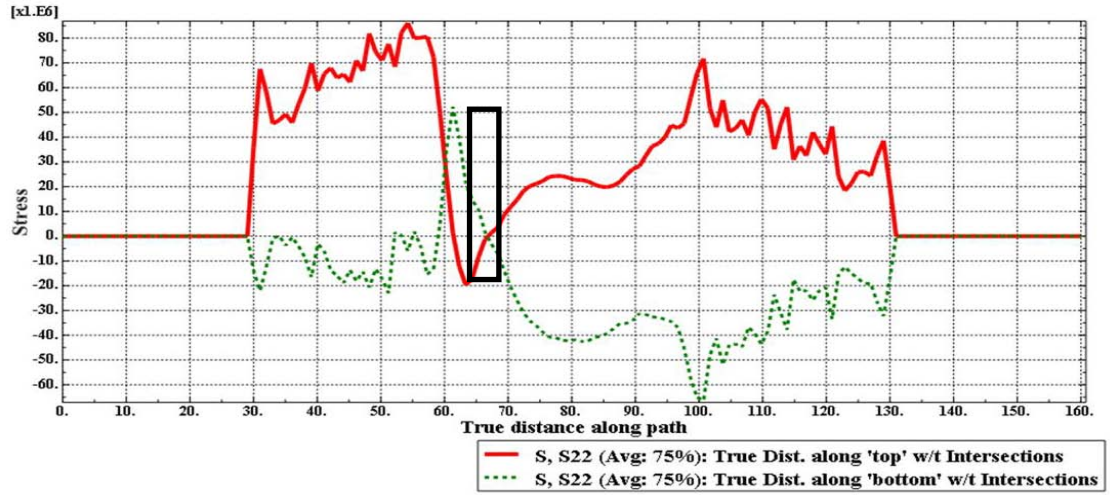

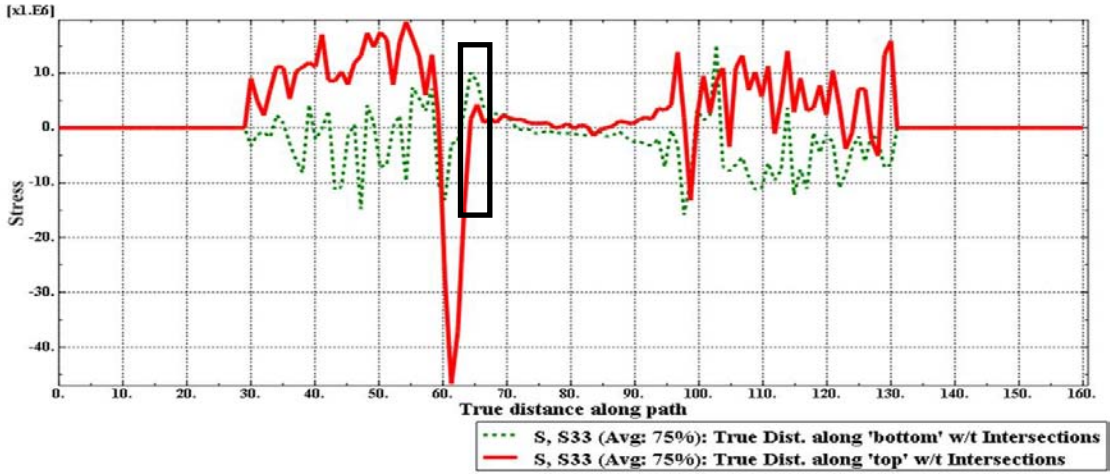

Figure 5.9: Stress variation along the 1.5mm thick sheet with a round tool radius of 10mm

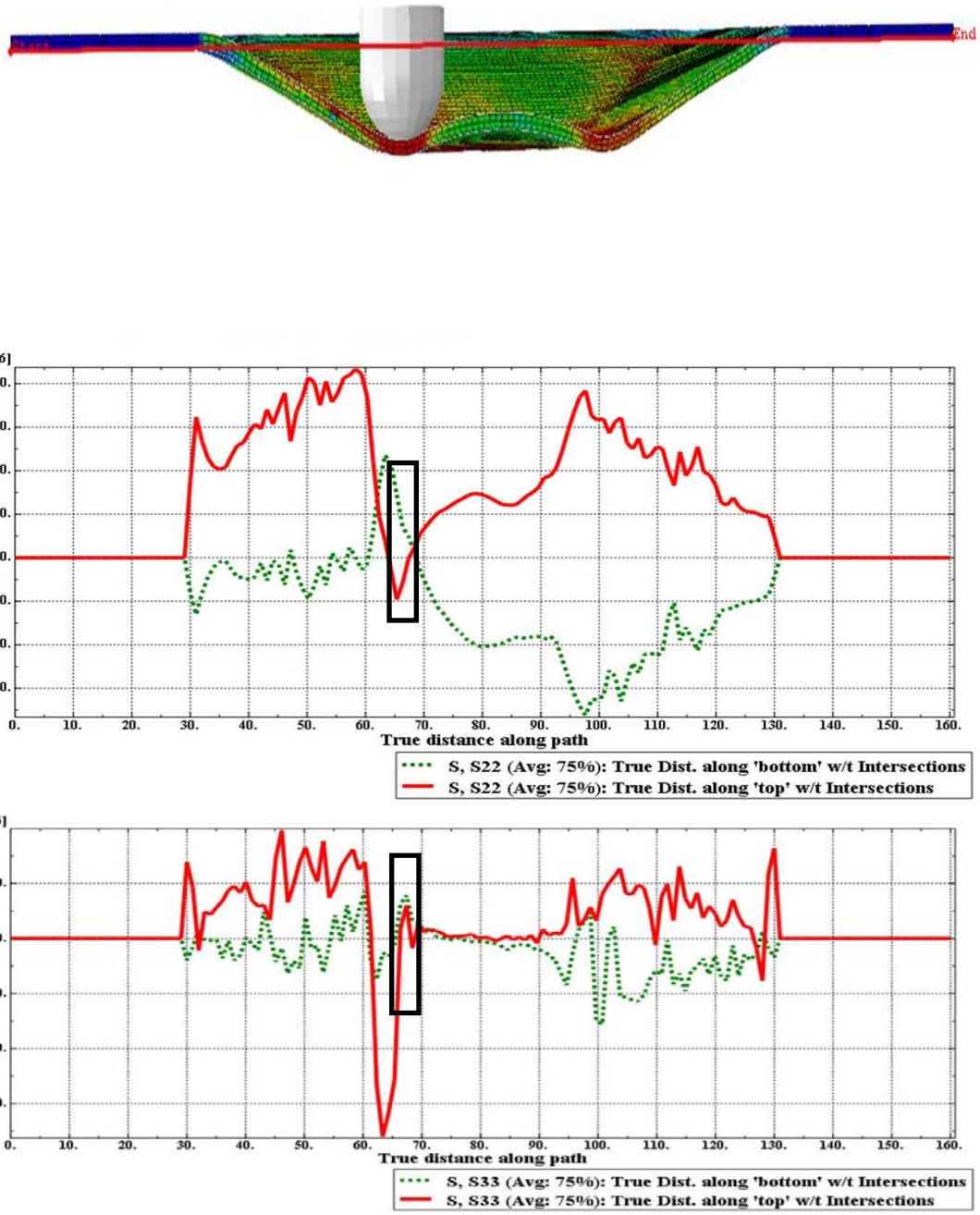

Figure 5.10: Stress variation along the 1.5mm thick sheet with a round tool radius of 14mm

The red continues lines shows the stress state on the top surfaces, while the green dotted lines show the stress states on the bottom surfaces. The black rectangles indicate the portion of the sheet along the profile just immediately by the tool in the direction perpendicular to the tool motion. Notice the reduction in the absolute values of the stress along the z plane at the center point of the tool.

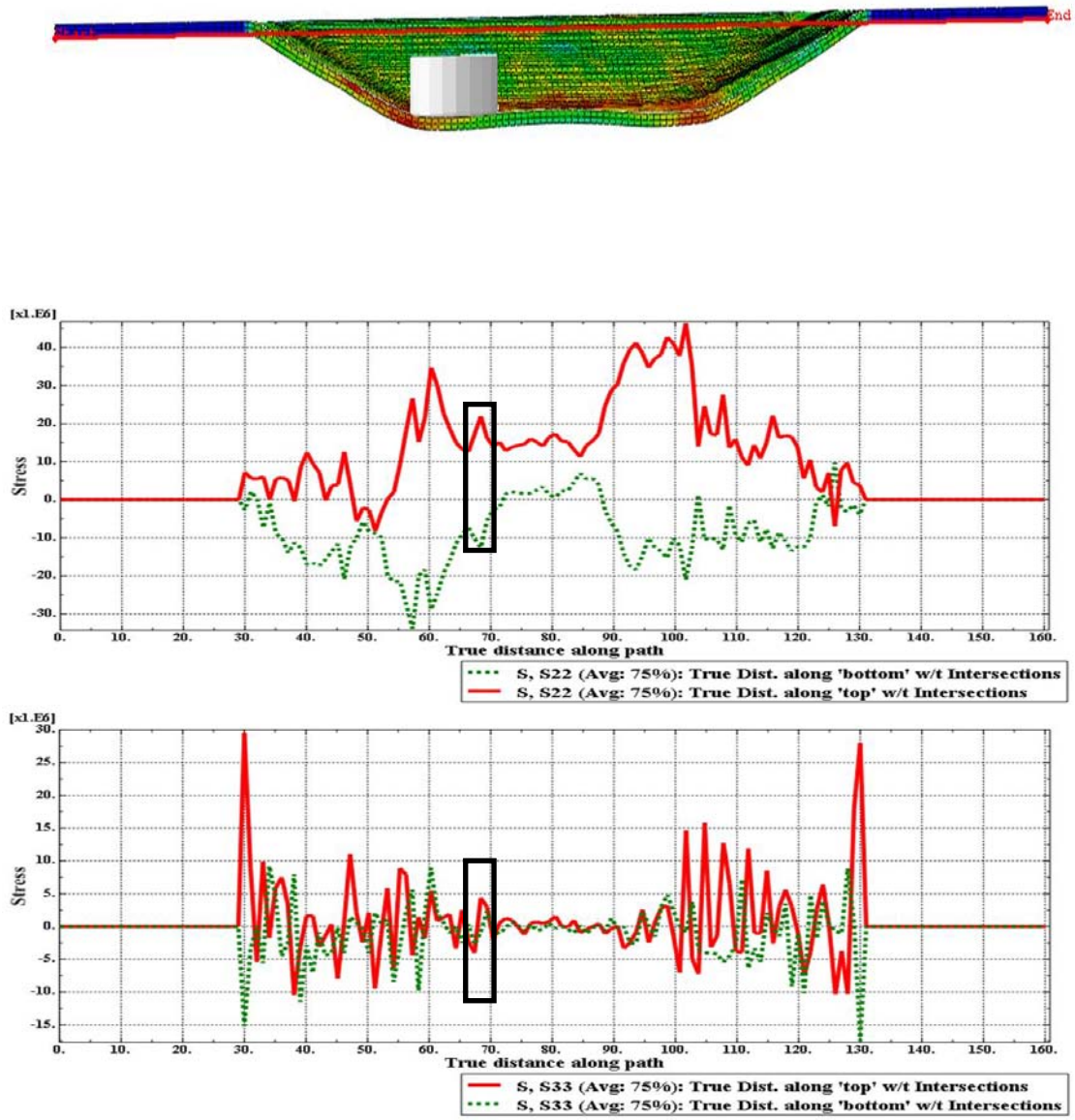

Figure 5.11: Stress variation along the 1.5mm thick sheet with a flat tool radius of 14mm

Notice that there exist tensile stresses on the top surface of the 14mm flat tool along s22, direction perpendicular to tool movement compared to the other stress diagrams. This shows that the material is undergoing stretching on the direction perpendicular to the movement of the tool. There exist little negative stresses in the z plane compared to the other simulations due to the low stresses applied by the flat tool with wide surface area.

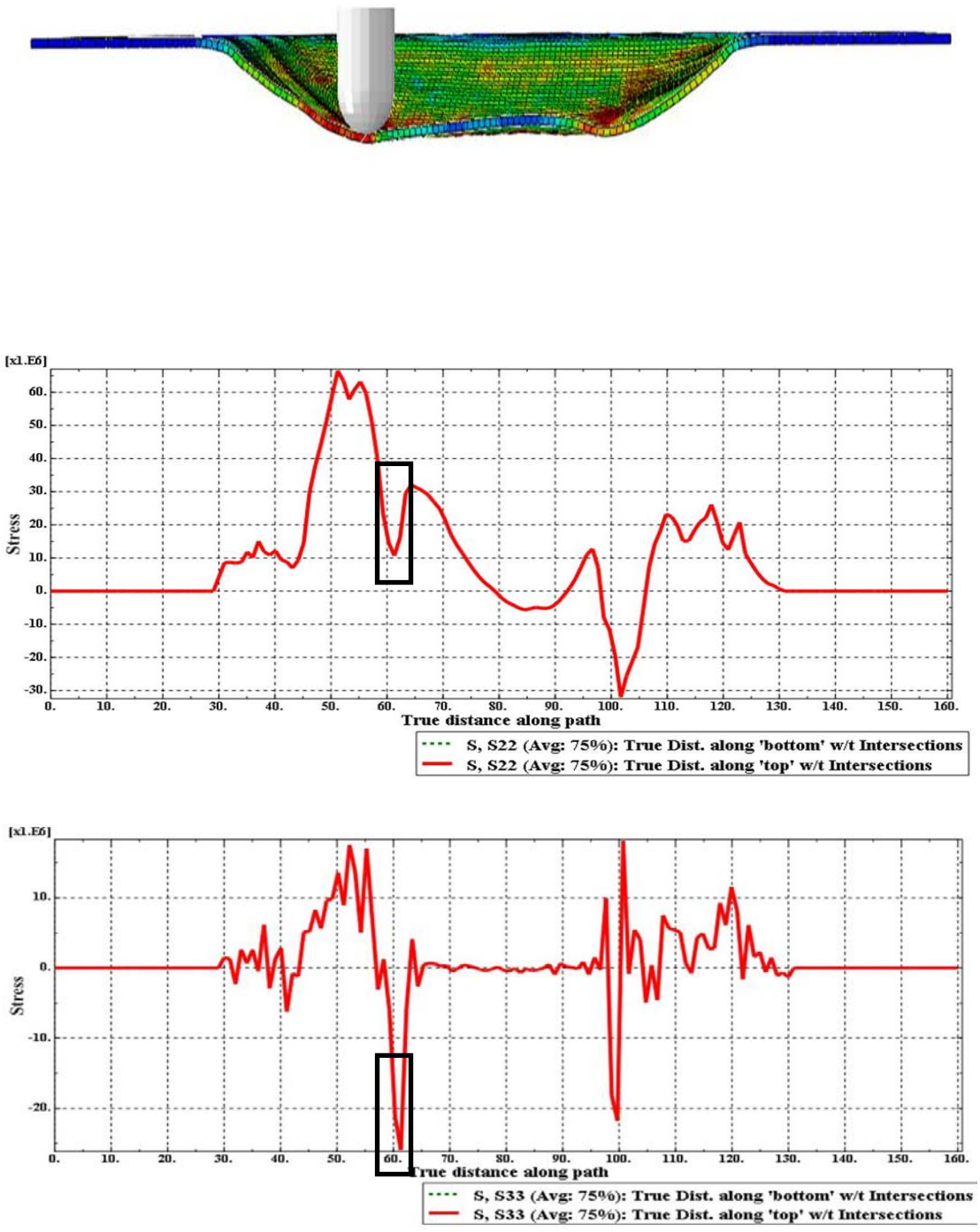

Figure 5.13: Stress variation along the 1mm thick sheet with a round tool radius of 10mm

For sheets with small thickness (1mm) the strain gradient along the thickness direction is small and there is no significant change in the stress state across the thickness. The stress and strain values obtained along the cut profile are same for both top and bottom surfaces. The stress state for the entire is similar to the stress

states in the bottom surface of a thicker sheet. In order to achieve better results for these simulations, smaller mesh elements could be defined in the simulation. However this would significantly add the computational time. These results further demonstrate the fact that pillow formation is caused by bending.

It should be noted that there is a significant change in the magnitude of stress and strain values at the point of contact between the tool and sheet for different tool sizes and geometries. Stress values become greater at the top surface as the tool radius is decreasing. Flat tools generally have lower stresses than the round tool. This is expected because of the highly localized stresses in the case of the round small tool. Due to the thickness of the sheet, stresses reduce towards the lower portion of the blank. The stress values in the case of the 1mm thick sheet being deformed by the round tool with10mm radius is less than the 1.5mm thick sheet being deformed by the same tool. Strain values too follow the same pattern for all the simulations.

From the above FEA analyses, it has been proven that pillow formation in SPIF is caused mainly by bending forces induced on the blank by the forming tool. The ratio of the tool size to sheet thickness is very important as this determines the amount of bend severity. Bend severity is thus a major parameter in the formation of pillow at the center of the blank.

In the following diagrams P.E 11 stands for strains along the tool movement direction (X), P.E 22 for strains perpendicular to tool movement (Y) and P.E 33 stands for strain in the depth direction (Z).

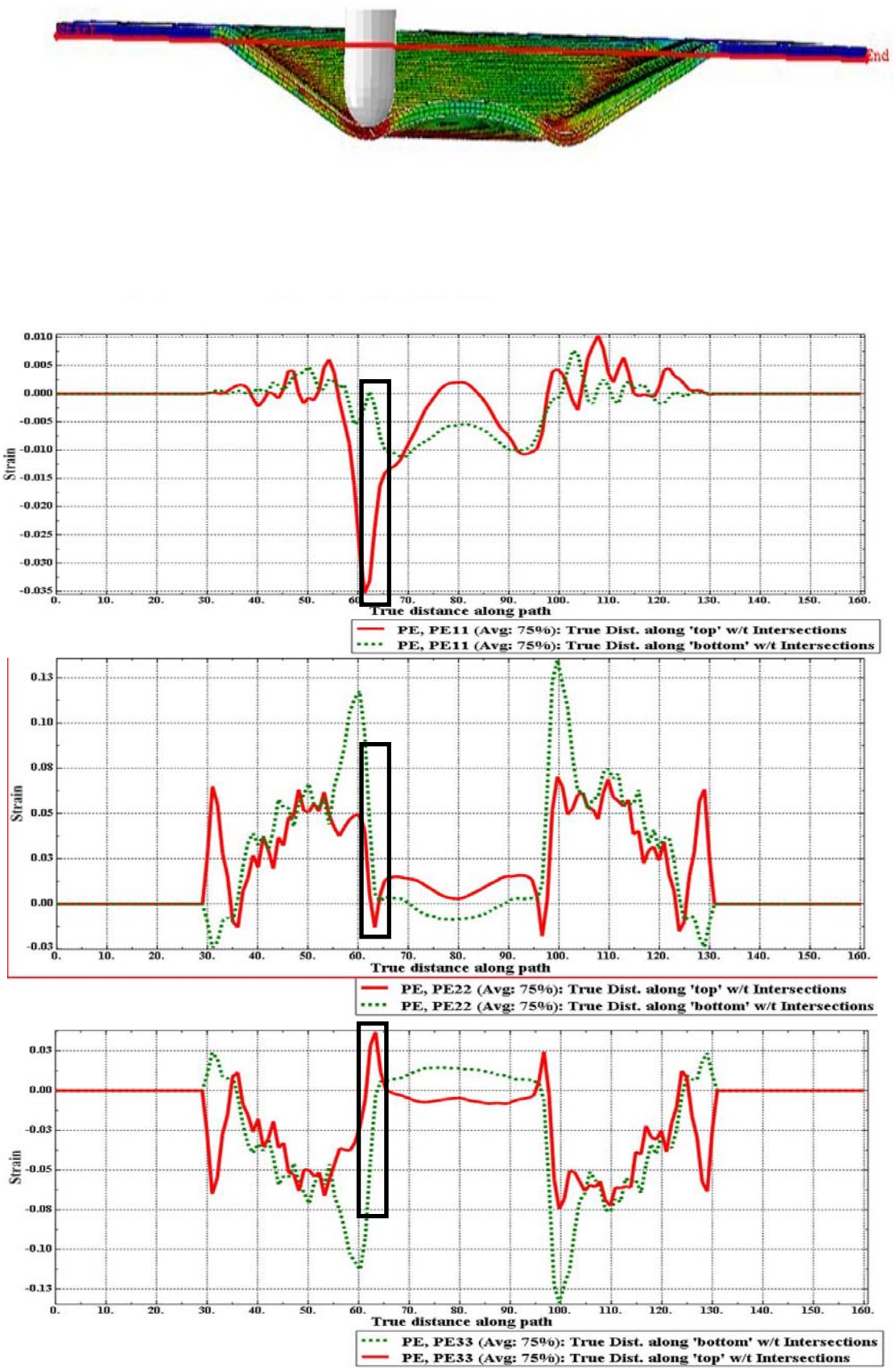

Figure 5.14: Strain variations along the 1.5mm thick sheet with a round tool radius of 10mm

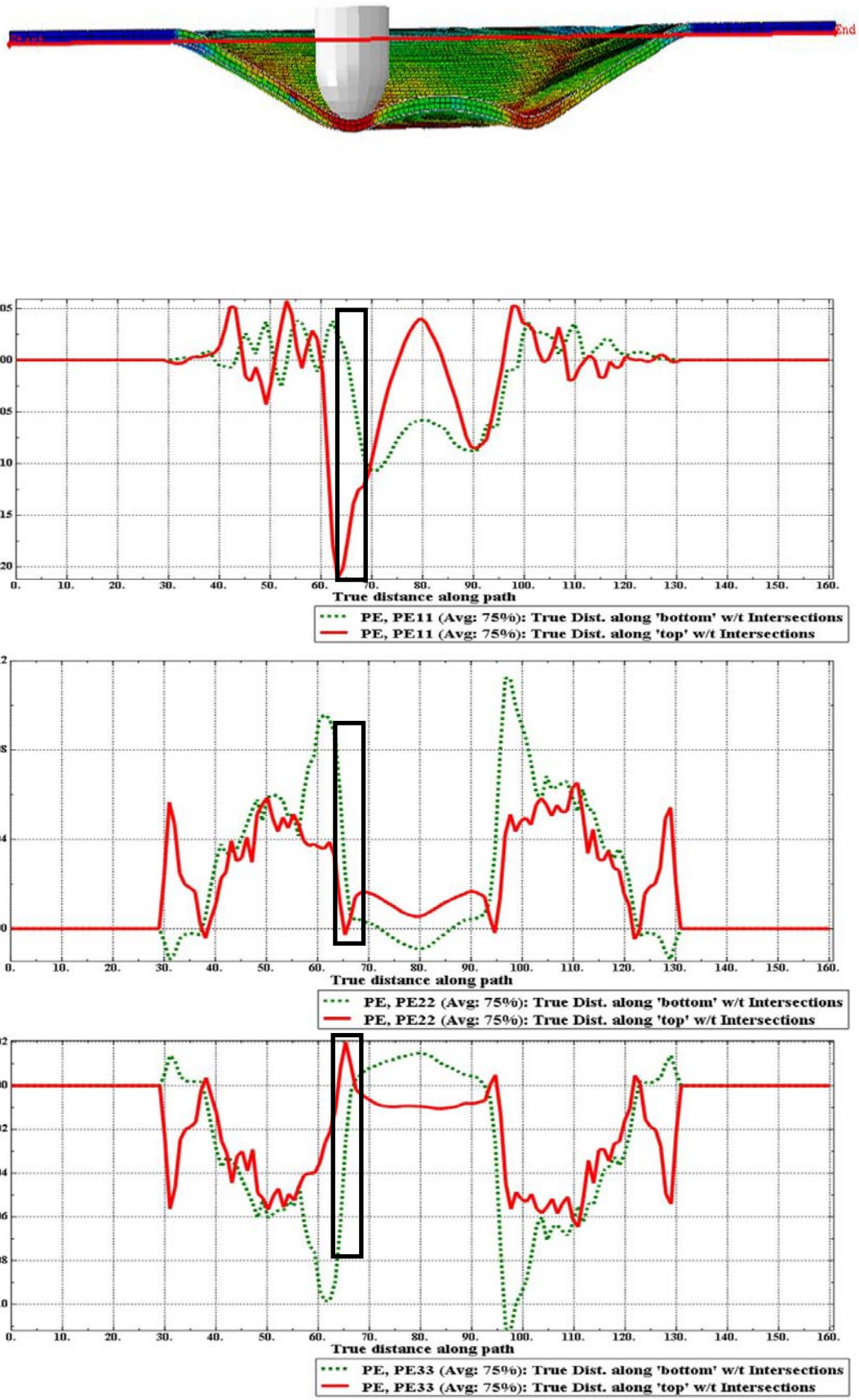

Figure 5.15: Strain variations along the 1.5mm thick sheet with a round tool radius of 14mm

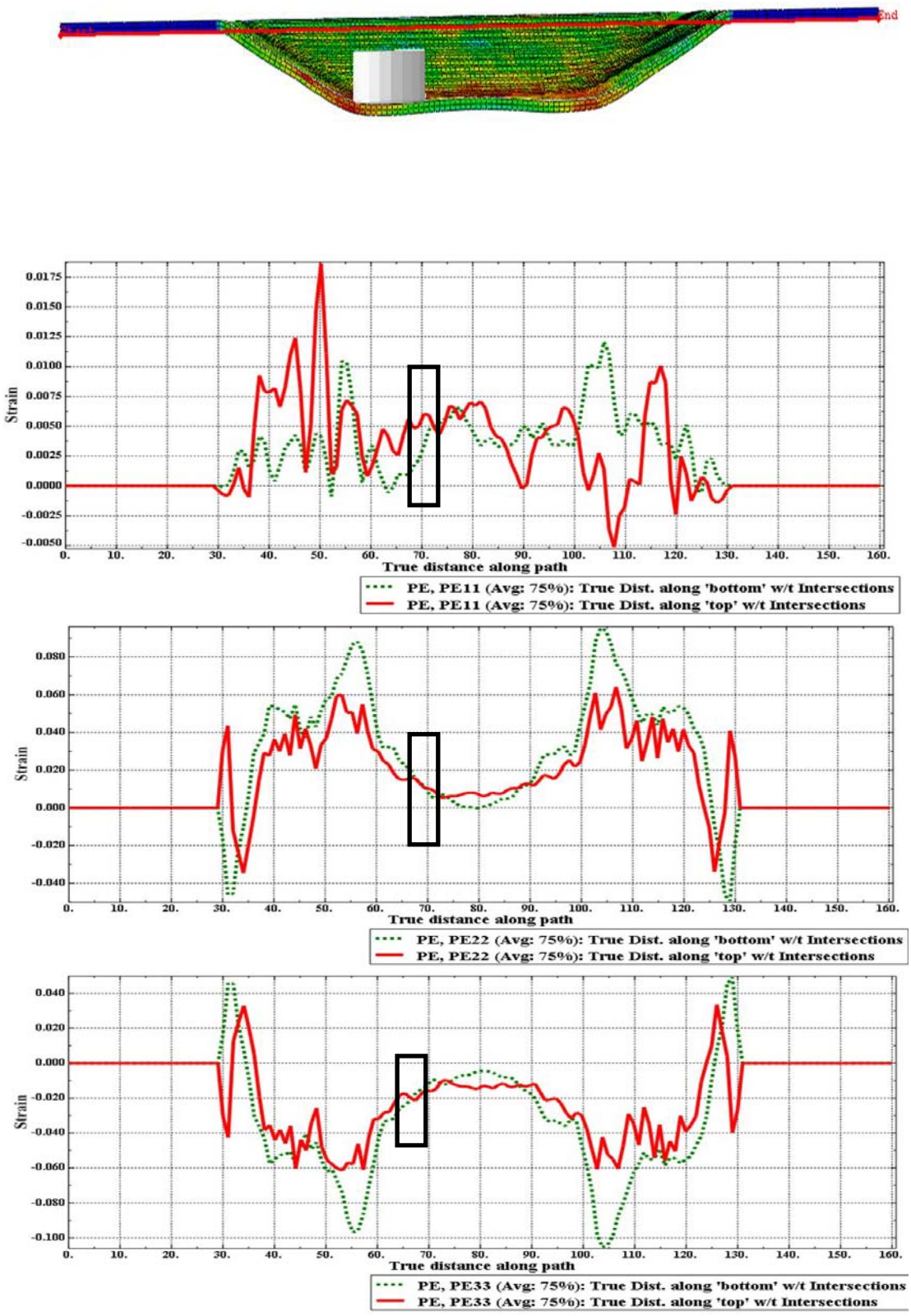

Figure 5.16: Strain variations along the 1.5mm thick sheet with a flat tool radius of 14mm

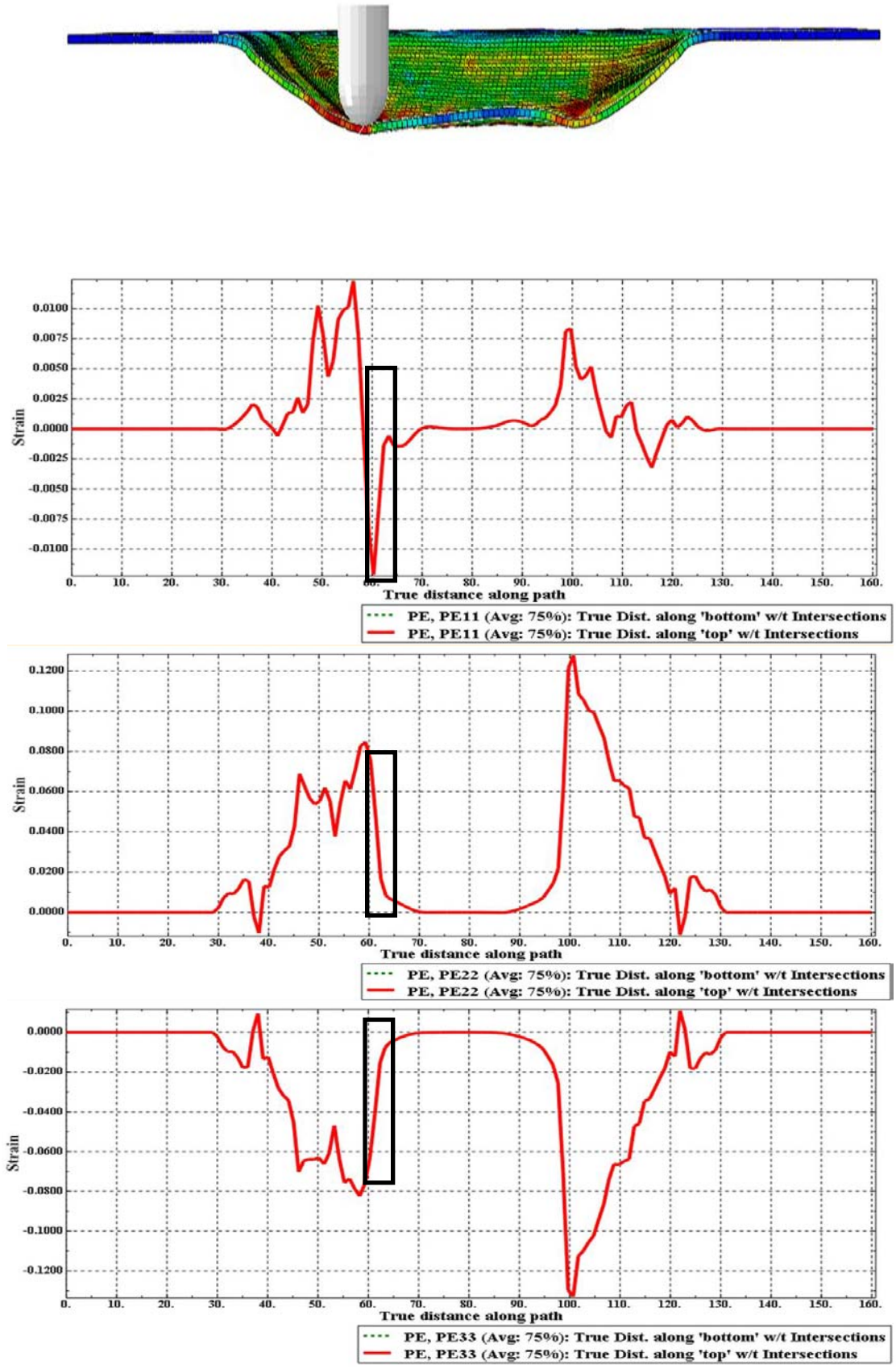

Figure 5.17 Strain variations along the 1 mm thick sheet with a round tool radius of 10mm.

Flats tools tend to form lower pillows than round tools. This may be due to lower bending angles and also the fact that flat tools may bend the sheet at two points along the profile. However, highly localized deformation at the point of contact between the flat tool and the part being formed causes early fracture because the tool tends to limit movement of the part material being formed from the bottom of the sheet to the walls.

Stretching of the sheet also occurs as the tool moves downward into the part. Thus pillow height reduces after a certain optimum height depending on process parameters. This can be demonstrated in FEA by positive tensile forces along the X and Y direction. This force decreases towards the center of the part and cannot compensate the bending force which actually causes pillow formation.

In the region close to the point of contact between the tool and the part, an increase in the original part thickness is noticed, this is taught to be caused by the tool preventing material flow from the bottom of the part to the formed wall. This has been noted as the compression zone by several authors, including (58). The geometry of the forming tool has a significant effect on this thickening, as smaller tools (lesser radius) cause more thickening than tools with large tool diameter. Some authors hold that is thickening is caused by compressive forces induced by the tool on the blank during the feed motion along the part depth. However, because pillow formation is accounted for by bending of the part rather than buckling and tensile rather than compressive forces act on the bottom surface of the sheet, it is safe to say this thickening is caused by friction which prevents material movement from the bottom to the wall of the formed part.

Chapter 6

CONCLUSION AND RECOMMENDATIONS

6.1 Conclusion

The research carried out in this M.Sc thesis was aimed at controlling pillow formation during SPIF. The experiments were carried out using flat and round tools of respectively 10 and 14mm cross sectional diameter, and a 20mm round tool. Annealed Aluminum sheets of 1 and 1.5mm thickness were used to carry out the experiment. The aluminum 1060 blanks were deformed to a depth of 12mm. The deformed area had dimensions 100x100mm.

As regards the influence of the tool geometry on pillow forming, the practical work and FEA both revealed that the pillow effect is more pronounced for the round tool than the flat tool and that pillow height reduces with an increase in the tool size.

It was observed that the 14mm flat tool produced the part with the least pillow while the 10mm round tool produced the part with the highest pillow.

FEA analysis helped in the determination of the kind of forces that act on the part as it is formed in SPIF. This leads to the conclusion that pillow formation in SPIF is caused primarily because of bending caused by the forming tool. Therefore, the degree of bend severity is the major parameter that determines pillow height.

Buckling could also some pillow formation but this is taught to have a lesser influence.

The main aim of this thesis was controlling pillow formation in SPIF however during the course of the study a proposed mechanism for pillow formation has been developed as given before.

6.2 Recommendations

Further works should investigate the influence of the forming speed, forming angle and temperature on pillow formation. In addition, means of countering the effects of the bending force on formed parts should be investigated in order to prevent pillow formation. The use of hydrostatic force or a vacuum to prevent bulge formation could be considered in this regard.

REFERENCES

[1] Retrieved from: OECD/IEA. 2014 [Online] http://www.iea.org/.

[2] Sivanandini M., Dhami S.S. & Pabla B.S. (2012). Flow Forming Of Tubes-A Review. International *Journal of Scientific & Engineering Research. 3(5)*.

[3] Schäfer T. (2007). Verfahren zur Hämmernden Blechumformung mit Industrieroboter. *Institut für Industrielle Fertigung und Fabrikbetrieb der Universität Stuttgart*. (in German)

[4] Schäfer T., Schraft R.D. (2005). Incremental sheet metal forming by industrial robots. *Rapid Prototyping Journal. 11(5),* 278 – 286.

[5] Duflou J.R., Callebaut B., Verbert J. & De Baerdemaeker H. (2007). Laser Assisted Incremental Forming: Formability and Accuracy Improvement. *CIRP Annals - Manufacturing Technology. 56,* 273-276

[6] Male A.T., Li P.J., Chen Y.W. & Zhang Y.M. (2001). Flexible Forming of Sheet Metal using Plasma Arc. *Journal of Materials Processing Technology. 115,* 61-64.

[7] Jurisevic B., Karl K. & Mihael J. (2006). Water jetting technology: an alternative in incremental sheet metal forming. *International Journal of Advanced Manufacturing Technology. 31,* 18-23.

[8] Retrieved from CustomPartNet. [Online 2014]. http://www.custompartnet.com/wu/sheet-metal-forming

[9] Hagan E., Jeswiet J. (2003). A review of conventional and modern single point sheet metal forming method. *Journal of Engineering Manufacture. 217,* 213–22.

[10] Kopp R., Schulz J. (2002). Flexible Sheet Forming Technology by Double-sided Simultaneous shot peen forming. *Annals of CIRP. 51(1),* 195-198.

[11] Retrieved from GlobalSpec Inc. 2014 [Online] http://www.globalspec.com.

[12] Zhang S.H., Wang Z.R., Wang Z.T., Xu Y. & Chen K.B. (2004). Some New Features in the Development of Metal Forming Technology. *Journal of Materials Processing Technology. 151*, 39–47.

[13] Bambach M., Hirt G. & Ames J. (2004). Modeling of Optimization Strategies in the Incremental CNC Sheet Metal Forming Process. *Numiform– Proceedings of the 8th International Conference on Numerical Methods in Industrial Forming Processes,Columbus, Ohio.* 1969-1974.

[14] Capece M. F., Durante M., Formisano A. & Langella A. (2007). Evaluation of the maximum slope angle of simple geometries carried out by incremental forming process. *Journal of Materials Processing Technology. 194*, 145- 150.

[15] Cavallini B., Puigpinos L. (2006). Incremental sheet forming: new technology for the manufacture of sheet metal parts directly from CAD files. *Rapid Product Development*- RPD.

[16] Bambach M., Hirt G. & Ames J. (2004). Modeling of Optimization Strategies in the Incremental CNC Sheet Metal Forming Process. *Numiform – Proceedings of the 8th International Conference on Numerical Methods in Industrial Forming Processes, Columbus, Ohio.* 1969-1974.

[17] Jeswiet J. (2000). Incremental single point forming. *Proceedings of NSF Design and Manufacturing Research Conference.*

[18] Jadhav S. (2004).Basic Investigations of the Incremental Sheet Metal Forming Process on a CNC Milling Machine. *Institut für Umformtechnik und Leichtbau, Germany.*

[19] Yang T. J, Kim D.Y. (2000). Improvement of formability for the incremental sheet forming process. *International Journal of Mechanical Sciences. 42(1),* 1271-1286.

[20] Tanaka S., Nakamura T., Hayakawa K., Nakamura H. & Motomura K. (2005). Incremental Sheet Metal Forming Process for Pure Titanium Denture Plate. *Proceedings of the 8th International Conference on Technology of Plasticity – ICTP*. 135-136.

[21] Drishtikona I. (2009). Sheet Metal Stamping in Automotive Industry.

[22] Hussain G. , Gao L. , Hayat N. , Cui Z. , Pang Y.C. & Dar N.U. (2008). Tool and lubrication for negative incremental forming of a commercially pure titanium sheet. *Journal of Materials Processing Technology. 203,* 193-201.

[23] Jackson K.P., Allwood J.M. & Landert M. (2008). Incremental forming of sandwich panels. *Journal of Materials Processing Technology. 204,* 290-303.

[24] Franzen V., Kwiatkowski L., Martins P.A.F. & Tekkaya A.E. (2009). Single point incremental forming of PVC. *Journal of Materials Processing Technology. 209,* 462-469.

[25] Le V.S., Ghiotti A. & Lucchetta G. (2008). Preliminary Studies on Single Point Incremental Forming for Thermoplastic Materials. *11th ESAFORM Conference on Material Forming*, Lyon, France.

[26] Ji Y.H., Park J.J. (2008). Formability of magnesium AZ31 sheet in the incremental forming at warm temperature. *Journal of Materials Processing Technology. 201,* 254-358.

[27] Micari F., Ambrogio G. & Filice L. (2007). Shape and dimensional accuracy in single point incremental forming: state of the art and future trends. *Journal of Materials Processing Technology. 191,* 390–395.

[28] Jeswiet J., Micari F., Hirt G., Bramley A., Duflou J.R. & Allwood J. (2005) Asymmetric single point incremental forming of sheet metal. *CIRP Annals Manufacturing Technology. 54 (2),* 623–649.

[29] Bambach M., Taleb A.B. & Hirt G. (2009). Strategies to improve the geometric accuracy in asymmetric singe point incremental forming. *Production Engineering. Research and Development. 3,* 145–156.

[30] Ambrogio G., Costantino I., De Napoli L., Filice L., Fratini L. & Muzzupappa M. (2004). Influence of some relevant process parameters on the dimensional accuracy in incremental forming: a numerical and experimental investigation. *Mater Process Tech. 153,* 501-507.

[31] Hussain G., Gao L. & Dar N.U. (2007). An experimental study on some formability evaluation methods in negative incremental forming. *Journal of Materials Processing Technology. 186,* 45-53.

[32] Hussain G., Gao L., & Hayat N. (2011).Forming Parameters and Forming Defects in Incremental Forming of an Aluminum Sheet: Correlation, Empirical Modeling, and Optimization: Part A. *Materials and Manufacturing Processes. 26*. 1546–1553.

[33] Ambrogio G., Cozza V., Filice L. & Micari F. (2007). An analytical model for improving precision in single point incremental forming. *J. Mater. Process. Techno. 191,* 92-95.

[34] Jackson K., Allwood J. (2008). The mechanics of incremental sheet forming. *Mater. Process. Technology. 209,* 1158–1174.

[35] Tomita Y. (1994). Simulation of plastic instabilities in solid mechanics. *Appl. Mech. Rev. 47(6)*, 171.

[36] Fang Y., Lu B., Chen J., Xu D.K. & Ou H. (2014). Analytical and experimental investigations on deformation mechanism and fracture behavior in single point incremental forming. *Journal of Materials Processing Technology. 214*, 1503–1515

[37] Chakrabarty J. (2006). Theory of Plasticity. Butterworth-Heinemann.

[38] Xu Z., Gao L., Hussain G. & Cui Z. (2010). The performance of flat end and hemispherical end tools in single-point incremental forming. *Int J Adv Manuf Technol. 46*, 1113–1118

[39] Kim Y.H., Park J.J. (2002). Effect of process parameters on formability in incremental forming of sheet metal. *Mater Process-Technology. 130*, 42-46.

[40] Hussain G., Gao L., Hayat N. & Qijian L. (2007). The effect of variation in the curvature of part on the formability in incremental forming: An experimental investigation. *International Journal of Machine Tools & Manufacture. 47*, 2177-2218.

[41] Ham M., Jeswiet J. (2007). Forming Limit Curves in Single Point Incremental Forming. *Mechanical and Materials Engineering, Queen's University, Kingston, ON, Canada*. *CIRP Annals. 56*, 277-280.

[42] Silva M.B., Skjoedt M., Atkins A.G., Bay N. & Martins P.A.F. (2008). Single-point incremental forming and formability-failure diagrams. *The Journal of Strain Analysis for Engineering Design. 43,* 15-35

[43] Silva M.B., Skjoedt M., Atkins A.G., Bay N. & Martins P.A.F. (2008). Revisiting the fundamentals of single point incremental forming by means of membrane analysis. *International Journal of Machine Tools & Manufacture. 48,* 73-83

[44] Capece M.F., Durante M., Formisano A. & Langella A. (2007). Evaluation of the maximum slope angle of simple geometries carried out by incremental forming process. *Journal of Materials Processing Technology. 194,* 145- 150.

[45] Hussain G., Gao L., Hayat N. & Qijian L. (2007). The effect of variation in the curvature of part on the formability in incremental forming: An experimental investigation. *International Journal of Machine Tools & Manufacture. 47,* 2177-218.

[46] Hussain G., Dar N.U., Gao L. & Chen M.H. (2007). A comparative study on the forming limits of an aluminum sheet metal in negative incremental forming. *Journal of Materials Processing Technology*. 187, 94-98.

[47] Park J.J., Kim Y.H. (2003). Fundamental studies on the incremental sheet metal forming technique. *Journal of Materials Processing Technology. 140,* 447-453.

[48] Silva M.B., Skjoedt M., Atkins A.G., Bay N. & Martins P.A.F. (2008). Single-point incremental forming and formability-failure diagrams. *The Journal of Strain Analysis for Engineering Design. 43,* 15-35.

[49] Wu S.H., Ana R., Andrade P.F.M., Abel D.S. & da Rocha B.A. (2012). Study of tool trajectory in incremental forming. *Advanced Materials Research. 472,* 1586-159.

[50] Fratini L., Ambrogio G., Lorenzo R.D., Filice L. & Micari F. (2004). Influence of mechanical properties of the sheet material on formability in single point incremental forming. *CIRP Annals – Manufacturing Technology. 53,* 207-210.

[51] Jeswiet J., Micari F., Hirt G., Bramley A., Duflou J.R. & Allwood J. (2005). Asymmetric single point incremental forming of sheet metal. *CIRP Annals Manufacturing Technology. 54(2),* 623–49.

[52] Micari F., Ambrogio G. & Filice L. (2007). Shape and dimensional accuracy in single point incremental forming: state of the art and future trends. *Journal of Materials Processing Technology. 191,* 390–5.

[53] Kopac J., Kampus Z. (2005). Incremental sheet metal forming on CNC milling machine tool. *Journal of Materials Processing Technology.162,* 622-628.

[54] Wu S.H., Ana R., Andrade P.F.M., Abel D.S., & Barata da Rocha A. (2012). Study of tool trajectory in incremental forming. *Advanced Materials Research. 475,* 1586-159.

[55] Ambrogio G., Costantino I., De Napoli L., Filice L., Fratini L. & Muzzupappa M. (2004). Influence of some relevant process parameters on the dimensional accuracy in incremental forming: A numerical and experimental investigation. *Journal of Materials Processing Technology. 153,* 501-507.

[56] Matthieu R., Jean-Yves H., Jean-Christophe H. & Yannick P. (2009). Tool path programming optimization for incremental sheet forming applications. *Computer-Aided Design. 41,* 877-885

[57] Skjoedt M., Hancock M.H. & Bay N. (2007). Creating helical tool paths for single point incremental forming. *Key Engineering Materials. 344,* 583–590.

[58] Martins P.A.F., Skjoedt N. & Silva M.B. (2008). Theory of single point incremental forming. *Journal of Strain Analysis. 43,*15-35.

[59] Ham M., Jeswiet J. (2006). Single point incremental forming and the forming criteria for AA3003. *CIRP Annals. 55,* 241-244.

[60] Adeosun S.O., Balogun S.A. (2011). Effect of Recrystallization Temperature and Time on the AA1060 Aluminum Alloy. *JOM. 63(5), 50-54.*

[61] Richelsen A.B. (1997). Elastic–plastic analysis of the stress and strain distributions in asymmetric rolling. *Int. J. Mech. Sci. 39,* 1199.

[62] Fang B.L., Chen J., Xu D.K. & Ou H. (2014). Analytical and experimental investigations on deformation mechanism and fracture behavior in single point

incremental forming. *Journal of Materials Processing Technology. 214*, 1503–1515.

[63] Sena J.I.V., Valente R.A.F., Grácio J.J., Simões F.J.P. & Alves de Sousa R.J. (2009). Finite element analysis of incrementally formed parts. *Paper presented at the 7th Euromech Conference in Solid Mechanics, Lisbon, September* 7-11.

APPENDIX

Tool path for 10mm tool round and flat defining tool movement on the CNC machine obtained from power mill soft ware.

```
%
     G17  G21  G40  G49  G80
     G59 G90
     S0M3
     G0X0Y0Z10.M9
     X43Y43
     Z5.

     G1Z-1F500.
     X-43
     Y-43
     X43
     Y43
     X42.534Y42.534

     Z-2
     X-42.534
     Y-42.534
     X42.534
     Y42.534
     X42.068Y42.068

     Z-3
     X-42.068
     Y-42.068
     X42.068
     Y42.068
     X41.602Y41.602

     Z-4
     X-41.602
     Y-41.602
     X41.602
     Y41.602
     X41.136Y41.136

     Z-5
     X-41.136
     Y-41.136
     X41.136
     Y41.136
     X40.670Y40.670

     Z-6
     X-40.670
     Y-40.670
     X40.670
     Y40.670
     X40.204Y40.204

     Z-7
     X-40.204
     Y-40.204
     X40.204
     Y40.204
     X39.738Y39.738

     Z-8
     X-39.738
     Y-39.738
     X39.738
     Y39.738
     X39.272Y39.272

     Z-9
     X-39.272
     Y-39.272
     X39.272
     Y39.272
     X38.806Y38.806

     Z-10
     X-38.806
     Y-38.806
     X38.806
     Y38.806
     X38.340Y38.340

     Z-11
     X-38.340
     Y-38.340
     X38.340
     Y38.340
     X37.874Y37.874

     Z-12
     X-37.874
     Y-37.874
     X37.874
```

```
Y37.874

G0Z10.
Y270
M9
M2
```